https://dx.doi.org/10.1016/j.scs.2023.105142

Mitigating vulnerability of a multimodal public transit system for sustainable megacities: a real-time operational control method

Lin Zhang[a], *Min Xu*[b]*, *Shuaian Wang*[a]

[a] *Department of Logistics and Maritime Studies, Faculty of Business, The Hong Kong Polytechnic University, Hung Hom, Hong Kong*

[b] *Department of Industrial and Systems Engineering, The Hong Kong Polytechnic University, Hung Hom, Hong Kong*

Abstract

The multimodal public transit system (MPTS) has been recognized as a primary mobility support system for sustainable megacities. However, it is often vulnerable to various service disruptions, and the most severe circumstance is the interdependent cascading failures interacting among urban rail transit, bus transit, and road transit networks. The vulnerability of an MPTS against this severe failure, associated with extreme performances, limits the building of future resilient megacities. In this paper, a real-time operational control method based on the system emergency capability (SEC) is developed to block the dynamic unfolding paths of this severe failure considering network topology characteristics and dynamic evolution characteristics. This method is immediately available for real-time emergency control, while previous studies on qualitative optimization strategies cannot. Remarkably, a three-stage association design process is conducted to explore the most efficient SEC loading strategy, involved with multiple intertwined influential factors, including the target loading stations, loading time-step intervals, and loading interval length and loading strength. Finally, a case simulation is undertaken to indicate the adaptability of the proposed method. This work can provide critical insights into real-world emergency resource allocation and an underlying simulator with search direction knowledge for future intelligent algorithm-based optimal control.

Keywords: interdependent cascading failures; system emergency capability; public transit; vulnerability mitigations; sustainable megacities

∗ Corresponding author
E-mail address: zhang_lins@hotmail.com (L. Zhang); min.m.xu@polyu.edu.hk, xumincee@gmail.com (M. Xu); hans.wang@polyu.edu.hk (S. Wang)

1. Introduction

Megacities with developed economies and societies are often vulnerable to natural disasters, occasional incidents, or terrorist attacks because of the large-scale crowd management complexity. The outbreak of public health emergencies such as COVID-19 has further highlighted the importance of the urban resilience agenda covering known and emerging issues [1-3]. For instance, the extreme performances of various infrastructure networks against cascading failures have recently gained increasing attention in constructing a resilient urban lifeline system, including the interdependent channel-road networks [4], smart water networks [5], traffic networks [6-8], power grids [9], interdependent power-communication networks [10], and public transit networks [11-13]. Among various infrastructure networks, the multimodal public transit system (MPTS) operates as a primary mobility support system for sustainable megacities in the resilient urban lifeline system. For instance, in Nanjing, China, with a population of 9 million, around 6 million passenger journeys were made on public transit daily. The heavy reliance means that even limited-service disruptions caused by occasional incidents can lead to severe outcomes affecting many commuters.

In summary, the MPTS is often vulnerable to various service disruptions, and the most severe circumstance is the interdependent cascading failures interacting among urban rail transit, bus transit, and road transit networks because of the intertwining of failures across transit modes and in a single transit mode, as illustrated in Fig. 1 and described in detail in Section 2. The sudden large passenger flow caused by holidays, large-scale activities, bad weather, and other emergencies may interrupt the stable state of the MPTS. As a substantial external disturbance to the MPTS caused by people, it also may improve the complexity of urban emergency management, which has seldom been focused on by previous studies [14]. When a sudden large passenger flow is evacuated to the public transit infrastructure, the extreme scenario with interdependent cascading failures is triggered to impact not only the public transit but also the other transit on roads. This means that the public transit and road network environments are prone to congestion, leading to diminished comprehensive efficiency. This congestion further contributes to the accumulation of exhaust pollutants, ultimately impacting people's satisfaction with urban transportation and emergency management.

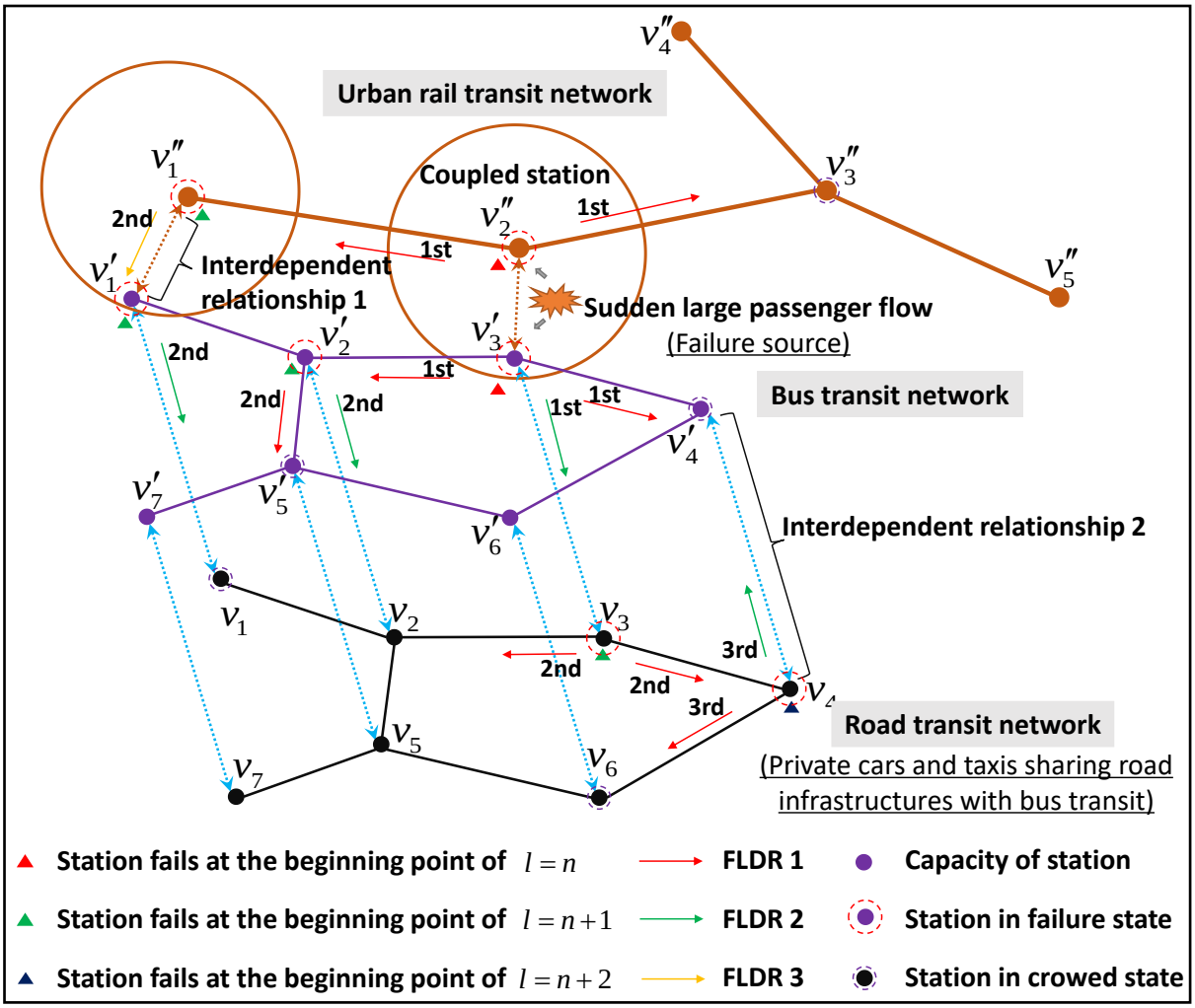

Fig. 1. Illustration of a general process of the interdependent cascading failures of an MPTS induced by a sudden large passenger flow. (Note: The station of the lower layer represents the road location corresponding to the bus transit station.)

Indeed, the vulnerability of an MPTS against this severe failure, associated with extreme performances, limits the building of future resilient megacities. This interdisciplinary research topic among urban science, network science, and transportation engineering provides a practical solution to quantify the entire reliability level for large-scale networks. Remarkably, it should be regarded as a special type of reliability at a network or system level, differing from runtime reliability quantification methods that can only apply to several routes or small-scale networks [15, 16]. However, current studies have seldom focused on the vulnerability of an MPTS against the interdependent cascading failures or have only focused on the vulnerability of a single transit mode (single urban rail transit or bus transit networks) against the independent cascading failures. More severely, most studies focused on modeling the unfolding process of cascading failures under various scenarios, thereby inferring some qualitative optimization strategies for long-term network designs. This type of optimization at a strategic level usually cannot be immediately available in real-world operations for real-time emergency

control but has a long-term effect on regulating operational behavior. Therefore, it is essential to develop a real-time operational control method to improve the comprehensive efficiency of sustainable public transit and road infrastructure for an emergency response when the interdependent cascading failures occur in an MPTS. Based on these understandings, this interdisciplinary research topic's logical evolution chain is proposed to highlight this paper's motivation, as shown in Fig. 2.

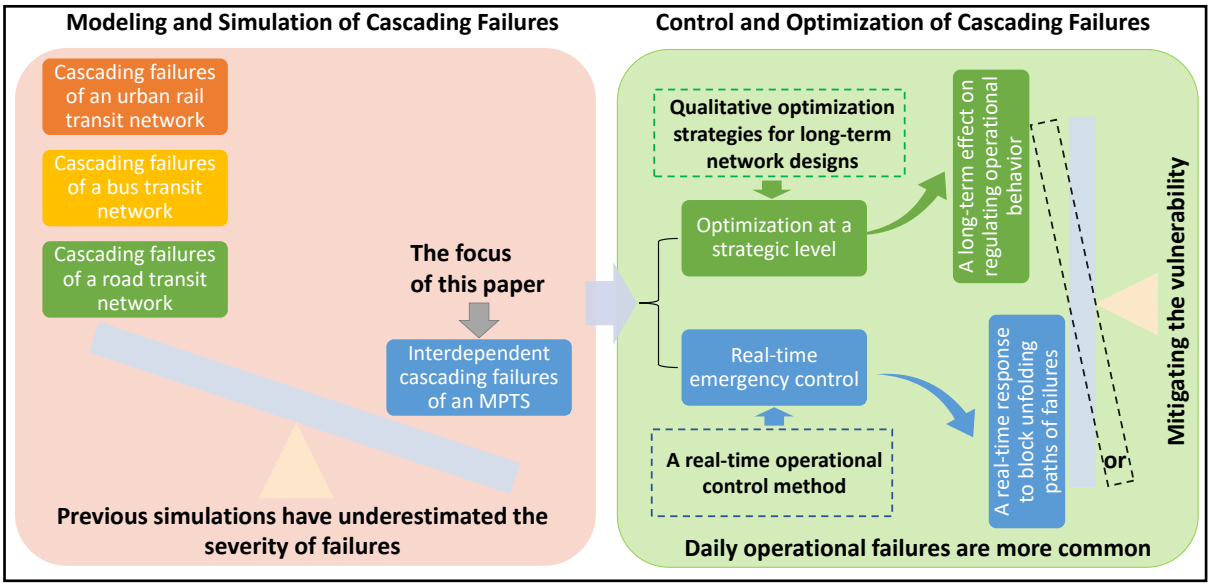

Fig. 2. The logical evolution chain of the interdisciplinary research topic.

1.1. Literature review

Cascading failures of public transit systems

Theoretically speaking, cascading failures, analyzed in complex networks, are a special dynamics process causing the collapse of a large portion of the network due to serious chain reactions among nodes. Due to the severe consequences of cascading failures in reality (e.g., the large-scale collapse event of power grids in North America in 2003 [17]), numerous scholars from different disciplines, including physics, reliability engineering, and transportation engineering, have conducted a series of studies on cascading failures of urban rail transit networks [12, 18-23], bus transit networks [24-26], and coupled urban rail transit-bus transit networks [11, 13, 27-30]. Unlike traditional studies focusing on the runtime reliability of several routes or small-scale networks [15, 16], the cascading failures of public transit systems are simulated to explore extreme performances. Most of these studies focused on modeling the unfolding process of cascading failures under various scenarios and identifying influential factors of cascading failures. However, less attention is paid to designing preventive and control strategies for cascading failures to mitigate the negative impacts. It is

worth mentioning that compared with urban rail transit or bus transit networks, studies on cascading failures of the coupled urban rail transit-bus transit network are rare due to the complexity of the coupled system. These limited studies lacked the consideration of transportation domain knowledge and were sometimes conducted under unrealistic assumptions. The most representative example is the neglect of the interaction effect with taxis, ride-hailing vehicles, and other private cars that share road infrastructures with bus transit. Recent work has recognized that this complex coupling dynamics among various public transit modes should be understood to reduce the gap between the model and reality. Zhang et al. recently proposed a cascading reliability model to model the unfolding of the interdependent cascading failures of an MPTS that is intertwined with three types of failure load dynamic redistributions (FLDRs) in a single layer and between layers [31].

Among some limited studies on cascading failure controls, the majority focused on the qualitative optimization strategies for long-term network designs at a strategic level, and rare attention is paid to real-time operational controls. For example, Jo et al. and Zhang et al. formulated FLDR rules considering various topological information and proposed optimization strategies for cascading failures [24, 30]. Zhang et al. simulated the cascading failure controllability by testing several control parameters of the cascading failure model, from which the parameters were abstracted from real-world optimization measures for operation management [31]. Shen et al. developed a station capacity assignment method to enhance network robustness [22]. Unlike the above studies, Huang et al. simulated cascading failures based on the disaster spreading theory and proposed five allocation strategies of the limited emergency resources for an urban rail transit network, and it was not a dynamic control for a time-step by time-step evolution process [20]. It is worth mentioning that these qualitative optimization strategies usually cannot be immediately available in real-world operations for cascading failure emergency control and are expected to have a delayed but long-term effect on regulating operational behavior. Similar to the purely model studies mentioned above, the existing cascading failure control studies did not address the interaction effect with taxis, ride-hailing vehicles, and other private cars that share road infrastructures with bus transit. This missing consideration causes the existing result to have a simplified coarse-grained description of network dynamics and low applicability to control the interdependent cascading failures of an MPTS.

Based on these understandings, the research gap in previous studies can be inferred as follows:

- **The preliminary inferred research gap.** A dedicated method for real-time operational controls should be developed to conduct real-time emergency response when the interdependent cascading failures of an MPTS occur.

Cascading failures of other paralleled real-world networks

The cascading failures of public transit systems are closely parallel to those of power grids and communication networks, which have been extensively investigated in the literature and can provide insights for real-time operational controls of the interdependent cascading failures of an MPTS. For example, some strategies based on the node failure repairing capability were proposed to reduce the vulnerability of power grids [32]. However, an MPTS does not have the so-called node repairing problem because failure stations under cascading failures are severely congested instead of suffering from permanent infrastructure damages. In other words, the failure loads of an MPTS remain in stations rather than being removed from the network caused by permanent infrastructure damages. Repairing failure stations after failure loads spread through them cannot reduce the evacuation pressure of failure loads. Besides, some recent studies have recognized that some reinforced nodes can resort to emergency plans or backup facilities to ensure function correctly [32-34]. While the reinforced node strategies can indeed impact the interdependent cascading failures of an MPTS, it is imperative to acknowledge that the reinforced nodes cannot be perennially exempted from succumbing to overload failures. This susceptibility is due to the inherent dynamism prevailing within the MPTS, which encompasses intricate human behaviors. Therefore, considering domain knowledge of transportation engineering, the key to conducting real-time control for the interdependent cascading failures of an MPTS is to improve the real-time processing capability of failure loads. More specifically, the system emergency capability (SEC) should be loaded to adjacent stations of failure stations before these adjacent stations receive the failure loads, thereby blocking the dynamic unfolding of cascading failures.

Based on the comparative analysis and experience reference with other paralleled real-world networks, the research gap summarized above should be further refined as follows:

- **The refined research gap.** The missing dedicated method should focus on improving the real-time processing capability of failure loads of various layers of an MPTS to block the dynamic unfolding of the interdependent cascading failures rather than to repair failure stations after the unfolded of cascading failures or reinforce stations.

1.2. Objective and contributions

To fill the research gap, this paper proposes a real-time operational control method to mitigate the interdependent cascading failures of an MPTS. That is, blocking this severe failure by appropriately loading the SEC to stations in the dynamic unfolding paths of cascading failures considering network topology characteristics and dynamic evolution characteristics. General interdependent cascading failures of an MPTS induced by a sudden large passenger flow are simulated based on the cascading reliability model proposed in the previous work [31] and are taken as the benchmark of real-time operational controls of cascading failures. First, inspired by the driving effects of topology on network dynamics, the SEC baseline value of each layer is determined based on the average capacity of stations in each layer. Then, the general SEC loading process is introduced. Furthermore, a three-stage association design process is conducted to explore the most efficient SEC loading strategy, involving multiple intertwined influential factors that incorporate the target loading stations, loading time-step intervals, and loading interval length and loading strength. Finally, a case simulation is undertaken to indicate the adaptability of the proposed method and to provide critical insights into real-world emergency resource allocation.

In summary, the contributions of this study lie in the following aspects:

- Enrichment of the connotation of controllability of cascading failures. The proposed SEC-based method is specifically designed to mitigate cascading failures from a real-time operational control perspective for real-time emergency control, which differs significantly from the traditional qualitative optimization strategies for long-term network designs at a strategic level. As a result, the panoramic controllability of the interdependent cascading failures of an MPTS can be realized by integrating these two aspects.
- Formulation of emergency management policies against cascading failures. The SEC loading mechanism is explored from the intertwining impacts of the target loading stations, loading time-step intervals, and loading interval length and loading strength. This advance is a crucial foundation for public transit managers in formulating efficient SEC loading strategies, thus providing insights to guide real-world emergency resource allocations.
- Guidance on the optimal control solution of cascading failures for large-scale networks. The proposed simulation-driven method is especially suitable for solving complex dynamic evolution problems of large-scale networks and provides an underlying

simulator with search direction knowledge and significant efficiency for intelligent algorithm-based optimal control.

The remainder of this paper is structured as follows: Section 2 introduces the general process of the interdependent cascading failures of an MPTS induced by a sudden large passenger flow. Section 3 formulates the general SEC loading process. Three groups of SEC loading strategies are designed in Section 4. In Section 5, a case simulation is conducted. Section 6 presents the conclusion and discusses future research directions.

2. The interdependent cascading failures of an MPTS

The cascading reliability model proposed in the previous work [31] can simulate the interdependent cascading failures of an MPTS and serves as the benchmark for real-time operational controls. Fig. 1 illustrates a general process of the interdependent cascading failures of an MPTS induced by a sudden large passenger flow, and this severe failure includes the cascading failures across layers and the cascading failures in a single layer. The three-layered topology, incorporating an urban rail transit network layer, a bus transit network layer, and a road transit network layer, is established by the modeling method of an MPTS [31] to consider both geographical adjacency and operational adjacency. For example, failures in the bus transit network can have a broader impact on stations of other transit modes that are not geographically but operationally adjacent to a given node. This impact is mainly due to the functionalities performed by the FLDR 2 and FLDR 1 in the lower layer. The time-step l is a special time scale characterizing the time length to complete one FLDR process, which consists of the beginning, middle, and end points for updating station load and state, transiting redistributed loads, and receiving redistributed loads, respectively. Following the general load-capacity model of cascading failures [37], stations are regarded as generating sources of loads, and edges are regarded as carriers to redistribute failure loads between adjacent stations. The initial load-capacity pattern of an MPTS is a stable state formed by a long-term game played by public transit managers to regulate the evolution of passenger travel demand. The previous cascading reliability model has included the corresponding pattern estimation method.

When a substantial external disturbance, such as a sudden large passenger flow, is input to the load-capacity evolution system, the failures of some key stations may interrupt the stable state because the gathered loads of these stations are much larger than their capacity. Then, severe chain reactions among stations may cause the collapse of a large portion or even the entire network, i.e., the interdependent cascading failures of an MPTS. Remarkably, the intertwining and coupling effect of three types of FLDRs drives the unfolding of cascading

failures until the load-capacity evolution system returns to a steady state (i.e., no FLDRs can occur). Table 1 summarizes the differences among three types of FLDRs, which helps to understand the dynamic unfolding of the interdependent cascading failures of an MPTS. The interactions among urban rail transit, bus transit, and road transit networks, incorporating both positive and potential negative effects, are performed by the FLDR 2 and FLDR 3 in the established nonlinear dynamics evolution system with a three-layered topology. Naturally, the emerging positive and potential negative effects after utilizing some control measures of cascading failures are also performed by the FLDR 2 and FLDR 3. These components contribute to a comprehensive understanding of the dynamics and resilience of the transportation system. In addition, the negative effects caused by preparing these control measures of cascading failures, such as the crowding impact on traffic's operations, can be performed by adding additional load on the related path.

Table 1. The differences among three types of FLDRs

FLDR type	Main dynamics	Interaction patterns	Dynamics in a time-step scale
FLDR following the user equilibrium rule (FLDR 1)	• It guides the failure load transiting between a failure station and its adjacent stations in each layer. • Due to the edge congestion effect, the redistribution of failure loads between a failure station and its adjacent stations is expressed as a dynamic game process.	• It is a one-way action rather than an interaction.	• It needs one full time-step to complete. • For one process of FLDR 1, the load and state of a failure station are updated at the beginning point of one time-step; then, the redistributed load from a failure station is transited at the middle point of this time-step, and is received by each adjacent station at the end point of this time-step.
Interaction considering the time-delay effect (FLDR 2)	• It guides the failure load interaction between the middle and lower layers. • Due to the time-delay effect, the redistribution of failure loads between a failure station and its interdependent station may be delayed for 0-2 time-steps and be received in 1-2 time-steps. • The interaction is exerted by an equivalent impact rather than a direct load conversion.	• The time delay effect of interdependent stations between the middle and lower layers is graded according to the distribution characteristics of topological characteristics of interdependent stations.	• It needs at least one full time-step to complete. • One process of FLDR 2 may be completed in 1-2 time-steps according to different grading of the time-delay effect. • At the single time-step scale, its process is the same as FLDR 1.

Interaction based on coupled stations (FLDR 3)	• It guides the failure load interaction between the middle and upper layers. • Due to the existing coupled station, the redistribution of failure loads between a failure station and its coupled station is immediately completed. • A direct load conversion exerts the interaction.	• The load converted between the bus transit and urban rail transit networks based on coupled stations is more convenient than that between bus transit and road transit networks, so FLDR 3 does not consider the time-delay effect.	• It is completed within the beginning point of one time-step because it does not have the process of transiting, receiving, and updating the converted load.

(Note: The FLDR models can be seen in the previous cascading reliability model [31].)

3. System emergency capability

3.1. Definition of the system emergency capability

Logically speaking, loading the SEC to a station is equivalent to temporarily increasing the capacity of this station, which is essentially a kind of system redundancy. In real-world operations, various infrastructures are often designed to be close to the required capacity with little redundancy to minimize construction costs [38]. This practice makes them sensitive to various emergencies, technical failures, service disruptions, extreme weather, and natural disasters. With the emphasis on infrastructure resilience, it is gradually recognized that adding some redundancy to various infrastructures is necessary for the subsequent reconstruction process. In this paper, a real-time operational control method based on the SEC is expected to mitigate the interdependent cascading failures of an MPTS by loading reasonable system redundancy.

Based on the above understanding, the SEC is defined as the processing capability of failure loads reserved for intervening in time before cascading failures spread to stations and participating in reducing the scale of failure loads. In theory, it is a kind of system backup and redundancy. In real-world operations, it corresponds to the traffic demand management capability enabled by the integrated use of various emergency plans and vehicles.

3.2. Determination of the system emergency capability

Determination of the SEC baseline value

The SEC baseline value refers to the fixed SEC assigned to a single station in the process against cascading failures, and it is also regarded as the minimum SEC assigned to a single station. In real-world operations, public transit managers generally determine the emergency response capability of various public transit modes according to the scale of network facilities

and passenger volumes [15]. Inspired by the driving effects of network topology on the network function and performance from a network science perspective, the SEC baseline value of each layer can be determined according to the respective capacity. Besides, this determination is caused by inherent characteristics of the load-capacity model of cascading failures, i.e., the dependency of complex evolutionary behavior of dynamic systems on the initial load-capacity pattern and heterogeneity of a network. Undoubtedly, determining it in this way rather than specifying a specific value can not only integrate the proposed SEC-based method into the research framework of the load-capacity model but also improve the adaptability of the proposed SEC-based method in various dynamic systems. Therefore, the SEC baseline values of the lower, middle, and upper layers in an MPTS, i.e., the $SEC_{baseline}^{lower}$, $SEC_{baseline}^{middle}$, and $SEC_{baseline}^{upper}$, are respectively formulated as follows:

$$\begin{cases} SEC_{baseline}^{lower} = \dfrac{\sum_{i=1}^{N^{lower}} C_{v_i}^{lower}}{N^{lower}} \\ SEC_{baseline}^{middle} = \dfrac{\sum_{i=1}^{N^{middle}} C_{v_i'}^{middle}}{N^{middle}} \\ SEC_{baseline}^{upper} = \dfrac{\sum_{i=1}^{N^{upper}} C_{v_i''}^{upper}}{N^{upper}} \end{cases}, \tag{1}$$

where N^{lower}, N^{middle}, and N^{upper} represent the number of stations in the lower, middle, and upper layers, respectively; $C_{v_i}^{lower}$ represents the capacity of station v_i in the lower layer; $C_{v_i'}^{middle}$ represents the capacity of station v_i' in the middle layer; $C_{v_i''}^{upper}$ represents the capacity of station v_i'' in the upper layer.

Determination of the total SEC considering control costs

The capability of complex networks against cascading failures can be maximized by optimally allocating limited resources while respecting cost constraints [39]. If the cost is not considered, the impact of cascading failures can be eliminated by deploying unlimited SEC. Therefore, to incorporate control costs overlooked in traditional studies, this paper introduces a constraint that the total SEC is assumed to be a positive integer multiple of the SEC baseline value. We also assume that the cost of assigning SEC to a single station is determined by the SEC volume. This approach enables a more comprehensive consideration of control costs involved in assigning SEC to stations and facilitates a more straightforward exploration of the

optimal SEC loading strategy. Furthermore, due to the existing significant differences among three layers in the station scale, topology, and impact from cascading failures, the total SEC of the lower, middle, and upper layers, i.e., the SEC_{total}^{lower}, SEC_{total}^{middle}, and SEC_{total}^{upper}, is respectively formulated as follows:

$$\begin{cases} SEC_{total}^{lower} = m_1 \cdot SEC_{baseline}^{lower} \\ SEC_{total}^{middle} = m_2 \cdot SEC_{baseline}^{middle} \\ SEC_{total}^{upper} = m_3 \cdot SEC_{baseline}^{upper} \end{cases}, \tag{2}$$

where m_1, m_2, and m_3 represent the control parameters that are comprehensively determined based on the failure load scale, dynamic evolution characteristics of cascading failures of each layer, and typical numerical simulation tests.

3.3. General SEC loading process

To block the dynamic unfolding of cascading failures, the SEC is loaded to some adjacent stations of the failure station before these adjacent stations receive the redistributed failure load. Fig. 3 shows the general SEC loading process in a simple network. More specifically, suppose the station v_i fails at the beginning point of time-step $l = n$ with the total failure load $L_{v_i, l=n}$. Its adjacent stations are the stations v_{j1}, v_{j2}, and v_{j3}, and its sub-adjacent stations are the stations v_{k1}, v_{k2}, v_{k3}, v_{k4}, and v_{k5}. In this case, the stations v_{j1} and v_{j3} are loaded with the SEC (which is regulated to be equal to the $SEC_{baseline}$ in each single loading process), thus causing the dynamic unfolding of cascading failures to be blocked at the station v_{j1} at the beginning point of time-step $l = n+1$; similarly, the sub-adjacent stations v_{k3} and v_{k4} are also loaded with the SEC.

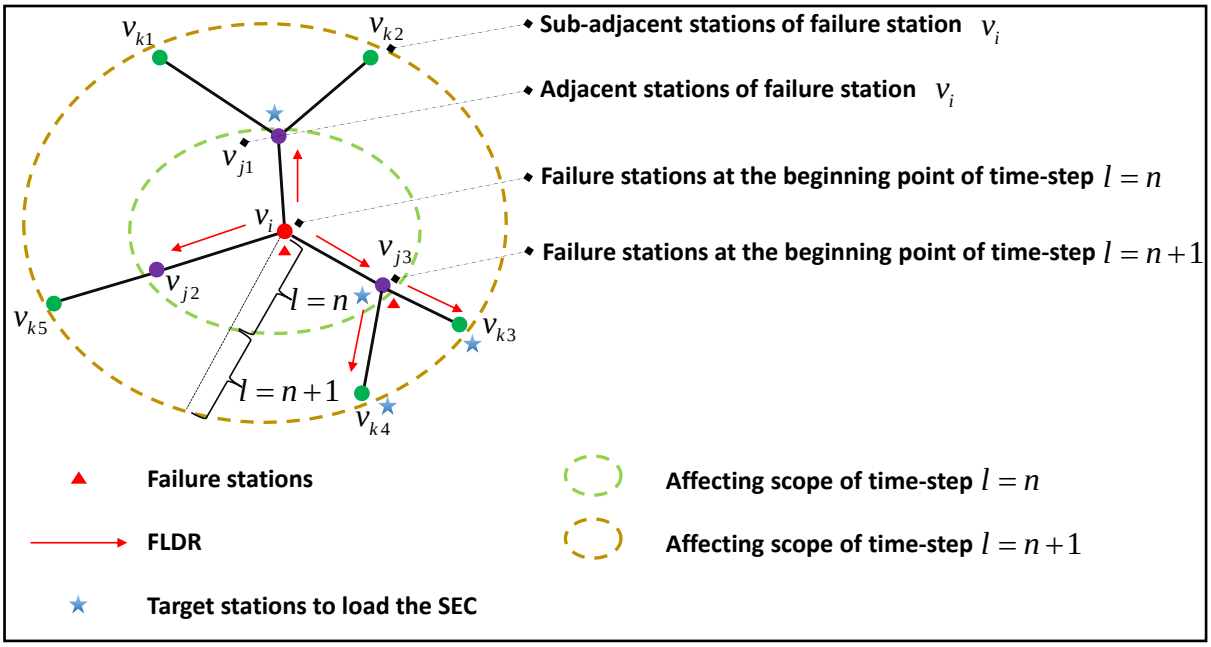

Fig. 3. Illustration of the general SEC loading process in a simple network.

Since the station v_{j3} will not only be loaded with the SEC in the time-step $l=n$ but will also become a failure station in the next time-step $l=n+1$, the dynamic updating process of its load is helpful in understanding the SEC action mechanism. Therefore, the carrying load of station v_{j3} at the beginning point of time-step $l=n+1$, represented by the $L_{v_{j3},l=n+1}$, satisfies the following equation:

$$L_{v_{j3},l=n+1} = L_{v_{j3},l=n} + \Delta L_{v_i \to v_{j3},l=n} - SEC_{baseline}, \tag{3}$$

where $\Delta L_{v_i \to v_{j3},l=n}$ represents the failure load redistributed from the failure station v_i to the adjacent station v_{j3} in the time-step $l=n$. Remarkably, inspired by Eq. (3), loading the SEC to a station is equivalent to removing some failure loads from the dynamic unfolding process of cascading failures. Unlike paralyzed loads with no path to continue being redistributed, these removed failure loads are shared by the added SEC and transformed into non-failure loads that cannot affect the unfolding of cascading failures. In other words, although loading the SEC to a station may not fully block cascading failures, it can reduce the total failure load to relieve the subsequent control pressure to a certain extent.

4. Loading strategy design of the system emergency capability

4.1. Principle of the proposed three-stage association design process

Generally, for each loading strategy, a single station is usually loaded with the SEC that is regulated to be equal to the $SEC_{baseline}$ during the process against cascading failures. The target

loading stations, loading time-step intervals, and loading interval length and loading strength of the SEC will integrate to block the dynamic unfolding of cascading failures. However, due to the complex and dynamic unfolding process of cascading failures, a three-stage association design process is conducted to explore the most efficient SEC loading strategy involved with the intertwined influential factors above. In the three-stage association design process, a loading strategy group is designed in each stage, and thus three loading strategy groups can gradually reduce the intertwined influential factors. Fig. 4 shows the framework of the proposed three-stage association design process for exploring the most efficient SEC loading strategy. Logically speaking, going from Group 1 to Group 2 and Group 3 is a process from a global perspective to two local perspectives, which aligns with the general logic for emergency resource allocation and the requirements for connecting with intelligent algorithms for accurate solving easily. The three stages are elaborated as follows:

- **First stage.** The target station to load the SEC in the single time-step scale is determined by the loading station-based strategies (Group 1), and this group is specifically explained and designed in subsection 4.2. In this group, the target (best) station to load the SEC in a single time-step can be identified in a loading interval with enough length time-steps. This loading interval, called the initial loading time-step interval selected by Group 1, incorporates many time-steps (each time-step is assigned the same and appropriate amount of the SEC) to test the loading station-based strategies.
- **Second stage.** The initial loading time-step interval selected by Group 1 is equally divided into three sections of equal length. This is to make sure the three subdivided time-step intervals have the same total SEC and loading strength of the SEC, and this group is specifically explained and designed in subsection 4.3. From the three subdivided time-step intervals, the target (best) time-step interval to load the SEC is further determined by the loading time-step interval-based strategies (Group 2).
- **Third stage.** Taking the best loading time-step interval identified by Group 2 as the loading time-step interval, the target (best) loading interval length and loading strength to block cascading failures are determined by the loading interval length and loading strength-based strategies (Group 3). This group is specifically explained and designed in subsection 4.4.

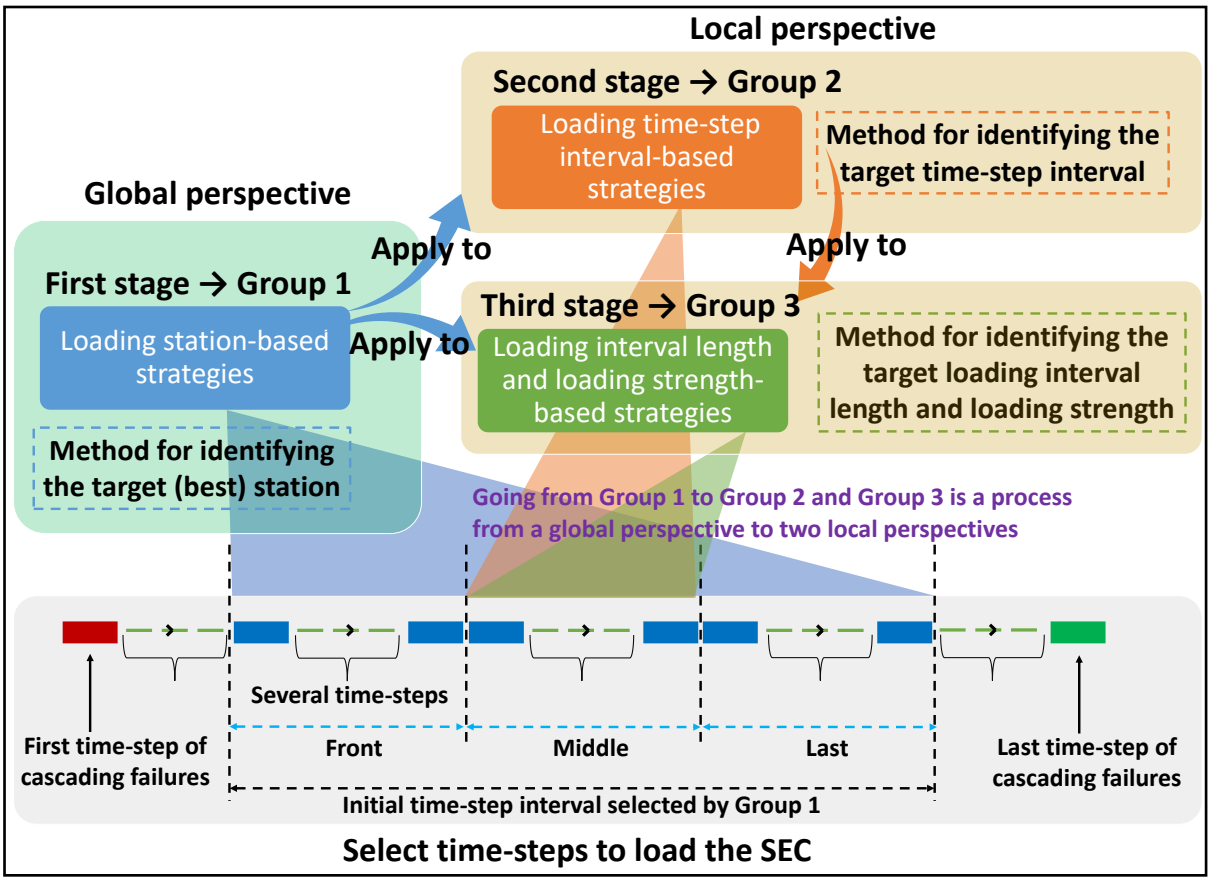

Fig. 4. The framework of the proposed three-stage association design process for exploring the most efficient SEC loading strategy.

4.2. Loading station-based strategies (Group 1)

In light of the impact of target loading stations on blocking the dynamic unfolding of cascading failures, the loading strategy group 1 is to identify the best loading way of a pre-specified number of target stations to load the SEC in the single time-step scale. We have proposed five loading station-based strategies of Group 1 in this section. Fig. 5 illustrates the difference among the five loading strategies of Group 1 in a single time-step, in which two stations are selected to load the SEC according to a judging perspective of the station importance driven by topology. The initial loading time-step interval of the SEC is chosen according to the dynamic evolution characteristics of cascading failures and typical numerical simulation tests. These loading strategies are elaborated as follows:

- **Loading Strategy 1-1 (LS 1-1):** For each layer, all adjacent stations of the failure stations identified at the beginning point of time-step $l = n$ are sorted in descending order regarding the station capacity. Then, the SEC loaded in the time-step $l = n$ should be assigned to the adjacent stations at the top of the ranking list of each layer.

- **Loading Strategy 1-2 (LS 1-2):** For each layer, all adjacent stations of the failure stations identified at the beginning point of time-step $l = n$ are sorted in ascending order regarding the station capacity. Then, the SEC loaded in the time-step $l = n$ should be assigned to the adjacent stations at the top of the ranking list of each layer.
- **Loading Strategy 1-3 (LS 1-3):** For each layer, all failure stations identified at the beginning point of time-step $l = n$ are sorted in descending order regarding the station capacity. Then, the SEC loaded in the time-step $l = n$ should be assigned to the adjacent stations of the failure stations at the top of the ranking list of each layer. For the ranked adjacent stations above, the SEC should be assigned to the adjacent stations with larger station capacity.
- **Loading Strategy 1-4 (LS 1-4):** For each layer, all failure stations identified at the beginning point of time-step $l = n$ are sorted in ascending order regarding the station capacity. Then, the SEC loaded in the time-step $l = n$ should be assigned to the adjacent stations of the failure stations at the top of the ranking list of each layer. For the ranked adjacent stations above, the SEC should be assigned to the adjacent stations with smaller station capacity.
- **Loading Strategy 1-5 (LS 1-5):** The SEC loaded in the time-step $l = n$ should be randomly assigned to adjacent stations of the failure stations in each layer.

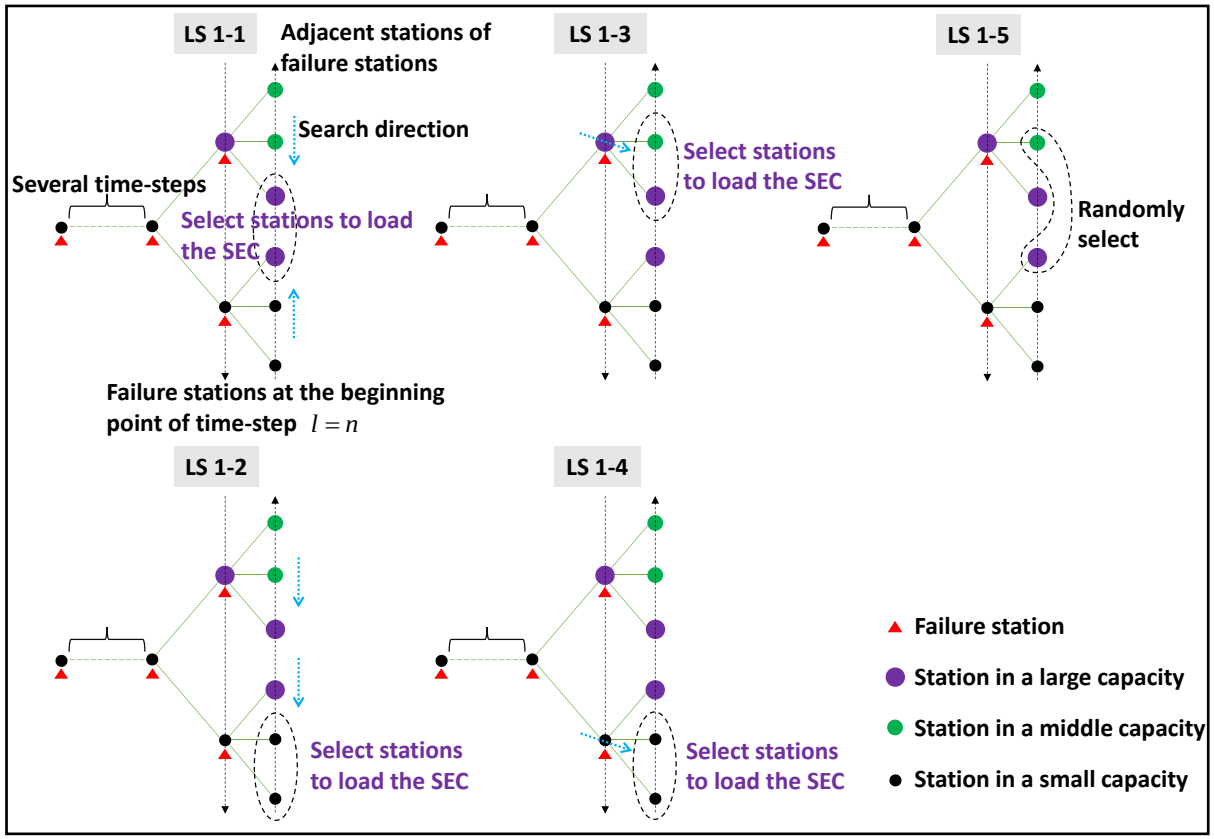

Fig. 5. Illustration of the differences among five loading strategies of Group 1 in a single time-step.

4.3. Loading time-step interval-based strategies (Group 2)

In light of the impact of target loading time-step intervals on blocking the dynamic unfolding of cascading failures, the loading strategy group 2 is to identify the best loading time-step interval to load the SEC. In this section, we have proposed three loading time-step interval-based strategies of Group 2. Fig. 6 illustrates the differences among the three loading strategies of Group 2. In this group, the initial loading time-step interval selected by Group 1 is equally divided into three sections of equal length, i.e., the subdivided time-step intervals of the front, middle, and last sections, referred to as the front, middle, and last time-step intervals, respectively. Only one subdivided time-step interval is selected to load the SEC, and the total SEC is set to one-third of that of Group 1 to maintain the same loading strength as Group 1 at the single time-step scale. The loading way in a single time-step of Group 2 is specified as the best loading way identified by Group 1. As a result, the three time-step intervals have the same total SEC and loading strength of the SEC. These loading strategies are presented as follows:

- **Loading Strategy 2-1 (LS 2-1):** The SEC is only loaded in the front time-step interval for each layer.
- **Loading Strategy 2-2 (LS 2-2):** The SEC is only loaded in the middle time-step interval for each layer.
- **Loading Strategy 2-3 (LS 2-3):** The SEC is only loaded in the last time-step interval for each layer.

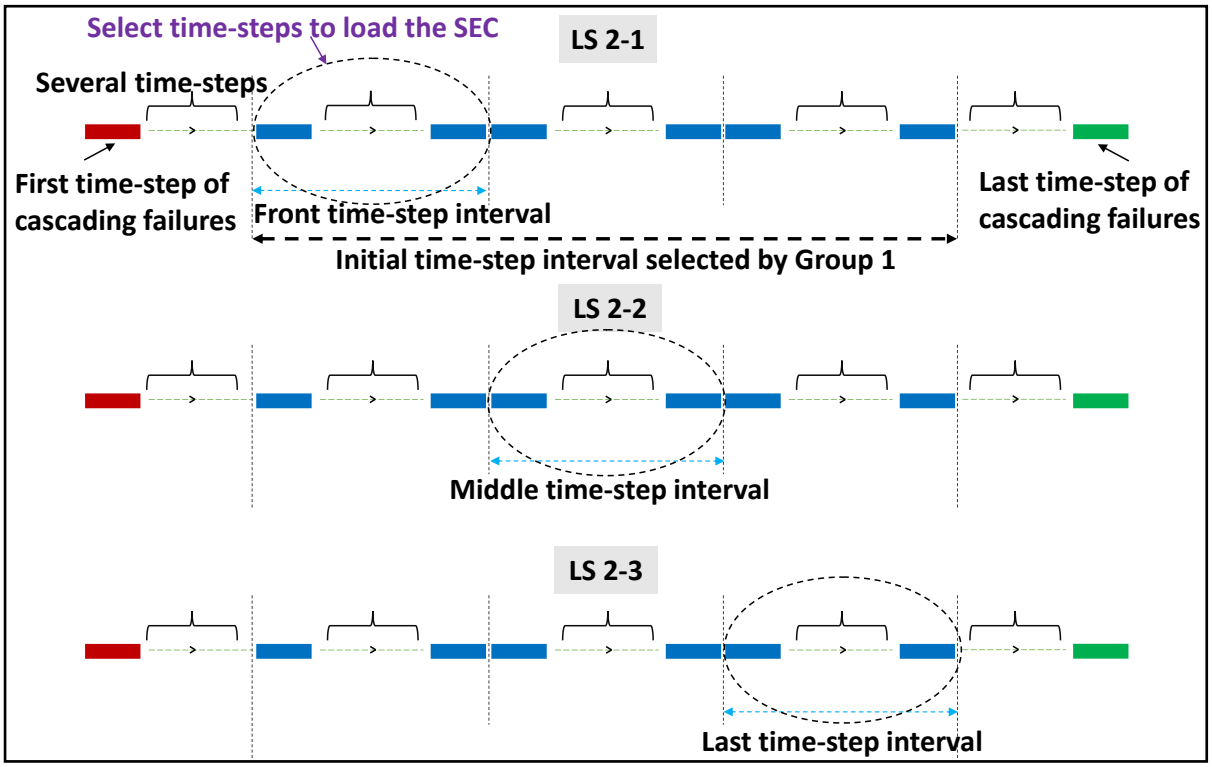

Fig. 6. Illustration of the differences among three loading strategies of Group 2.

4.4. Loading interval length and loading strength-based strategies (Group 3)

In light of the impacts of target loading interval length and loading strength on blocking the dynamic unfolding of cascading failures, the loading strategy group 3 is to capture a balance between loading interval length and loading strength. In this group, we have employed the best strategy of Group 2 as the baseline to design two loading interval length and loading strength-based strategies of Group 3. Fig. 7 illustrates the difference between the two loading strategies of Group 3, in which the loading time-step interval length of Group 2 is shortened by 50%, and the SEC that originally belongs to the last 50% time-steps is evenly loaded to the first 50% time-steps. As a result, the loading strategies of Group 3 can have the same total SEC as the benchmark strategy from Group 2 but double the loading strength of the SEC and shorten the loading interval length by half. This operation contributes to identifying the target loading interval length and loading strength. The target stations of the evenly loaded SEC above can be the 'planned stations' or 'unplanned stations'. Herein, the 'planned stations' are the selected stations determined by the loading strategy selected from Group 2 to load the SEC in the first 50% time-steps, and the other unselected stations are the 'unplanned stations'. For instance, the purple stations are the 'planned stations', and the green and black stations are the 'unplanned stations', as shown in Fig. 7.

- **Loading Strategy 3-1 (LS 3-1):** Developed from the loading strategy selected from Group 2, for each layer, the SEC that originally belongs to the last 50% of time-steps is loaded to the 'unplanned stations' in the first 50% time-steps.
- **Loading Strategy 3-2 (LS 3-2):** Developed from the loading strategy selected from Group 2, for each layer, the SEC that originally belongs to the last 50% of time-steps is loaded to the 'planned stations' in the first 50% time-steps.

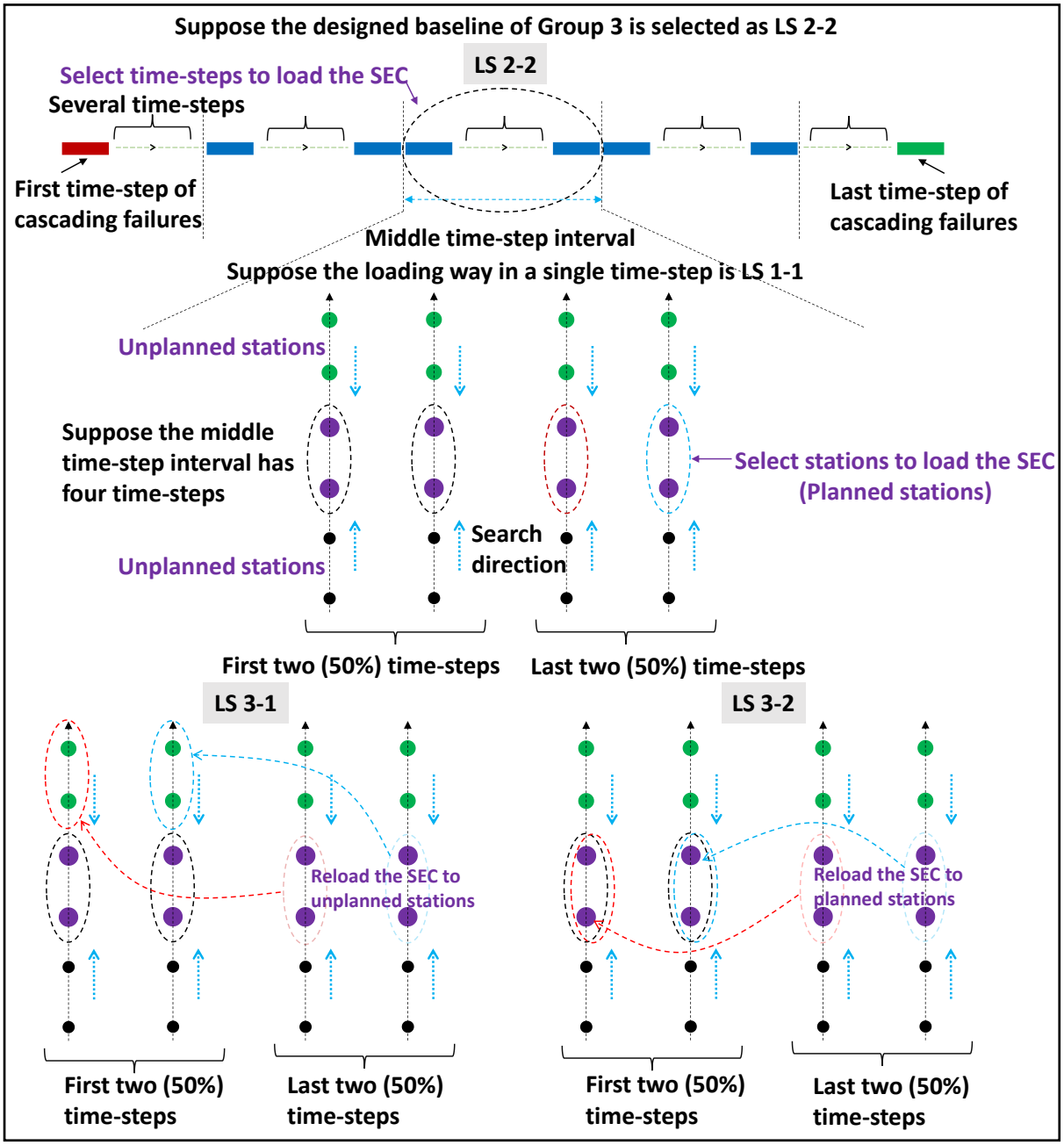

Fig. 7. Illustration of the differences between the two loading strategies of Group 3.

5. Case study

As one of the major cities in China, Nanjing has a large-scale MPTS and thus will be used in this section for the case study. The MPTS data were collected in December 2018, covering 411 bus transit routes and 3841 bus transit stations, as well as 10 urban rail transit routes and 122 urban rail transit stations. The data concerning the route and station layout, the route departure schedule, the vehicle marshaling form of urban rail transit routes, and the representative bus vehicle model are collected and utilized. The Nanjing Station, a large-scale integrated passenger hub station, is assumed to be the source of the interdependent cascading failures of an MPTS induced by a sudden large passenger flow. The operational map of Nanjing's MPTS is shown in Fig. 8.

Based on the previous work [31], the interdependent cascading failures of Nanjing's MPTS induced by a sudden large passenger flow from the Nanjing Station are described as a nonlinear dynamics evolution system with a three-layered topology. Theoretically, the sudden large passenger flow can be classified into large passenger flow caused by holidays, large-scale activities, bad weather, and other emergencies [40]. As this paper provides a generic methodology framework with wide applications, the scenarios of other shocks, such as infrastructure failure or fire accidents, can also be addressed. Infrastructure failures or fire accidents mainly lead to the network's capacity (supply) loss, while the sudden large passenger flow increases the network's load (demand). They have the same physical meaning under the modeling framework of interdependent cascading failures, and the main difference lies in the total failure load that they can transform and input into the MPTS to trigger the interdependent cascading failures. Consistent with the simulation initialization of the previous work [31], simulations are performed during weekday peak hours (7:00-9:00 a.m.). This is because the network performance during the selected time period is most representative, verified by the time-varying topology-based dynamics analysis in the previous work [41]. It is essentially the natural unfolding of cascading failures and should be taken as a benchmark to evaluate the performance of the proposed loading strategies. Based on the established nonlinear dynamics evolution system, the control roles of the proposed SEC loading strategies under the total SEC constraint are compared in the following subsections.

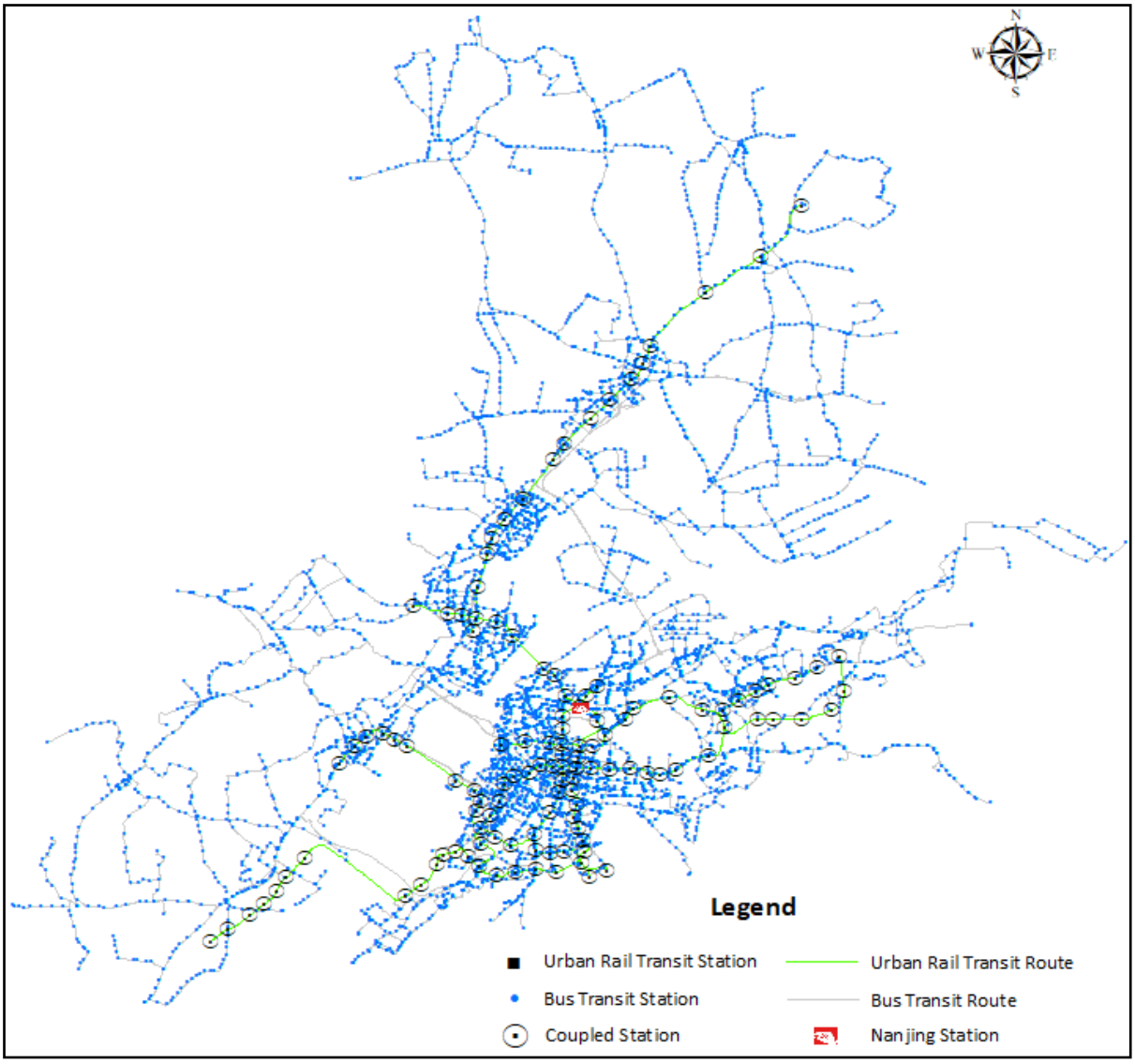

Fig. 8. The operational map of Nanjing's MPTS.

5.1. The control role simulation for the loading strategy group 1

In this subsection, the loading time-step interval to load the SEC is specified as $l \in [2, 25]$. In each time-step of this interval, one station of the lower layer, three stations of the middle layer, and one station of the upper layer are loaded with the SEC equal to the $SEC_{baseline}^{lower}$, $SEC_{baseline}^{middle}$, and $SEC_{baseline}^{upper}$, respectively.

Simulation results measured by RCF

RCF is the ratio between the number of failure stations and the number of stations in the MPTS. λ is the load tolerance parameter; λ_C is the threshold of the parameter λ, identified by observing that RCF drops sharply from the previous step and synchronously contrasts with other parallel evolutions; and the simulation interval $\lambda \in [0.05, 2]$ simulates

uncertain relationships between the station load and capacity. The smaller the RCF of a point, the greater the cascading reliability, and the λ_C follows the same rule.

Fig. 9 shows the control role simulation for the loading strategy group 1 measured by RCF, in which subfigures (b) and (c) are enlarged representations of subfigure (a). It can be observed that different loading strategies have different optimal applicable simulation intervals, and thus, it is necessary to explore the most efficient SEC loading strategy corresponding to varying real-time cases. More specifically, the LS 1-4 has the best control capability of the interdependent cascading failures outside the simulation interval $\lambda \in [0.75, 1.05]$, indicating that the SEC should be loaded to the adjacent stations with smaller capacity of the failure station with smaller capacity. In addition, although the LS 1-4 has the best control capability in most simulation intervals, the results show that $\lambda_c^{LS\ 1\text{-}4} > \lambda_c^{LS\ 1\text{-}3} = \lambda_c^{LS\ 1\text{-}1}$, i.e., the loading strategies designed based on the stations with larger capacity have the smaller (better) λ_c. This observation suggests that within a specific simulation interval $\lambda \in [\lambda_c^{LS\ 1\text{-}3}, \lambda_c^{LS\ 1\text{-}4}]$, the SEC should be loaded to the stations with larger capacity to control the spread of cascading failures rapidly.

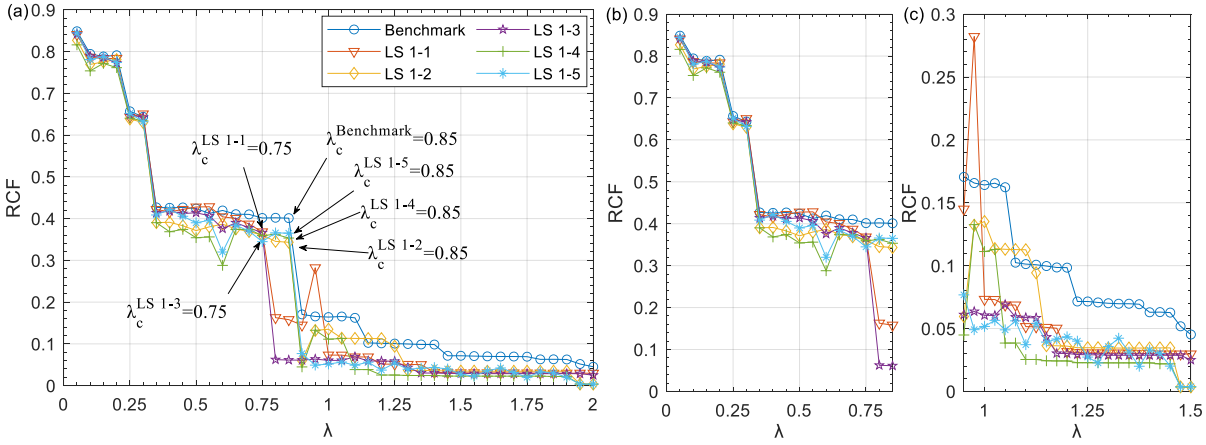

Fig. 9. Simulation results of the loading strategy group 1 measured by RCF.

Simulation results measured by $RTCF_{global,l=n}$

$RTCF_{global,l=n}$ is the ratio between the number of failure stations in the time-step $l=n$ and the number of stations in the MPTS. SUM is the sum of the z-axis values of a figure. SUM_κ is the sum of the z-axis values of the area κ of a figure (area κ follows $\lambda \in [0,2] \wedge l \in [20,30]$). Remarkably, the MPTS usually has the largest failure strength in the area κ. The smaller the $RTCF_{global,l=n}$ of a point, the greater the cascading reliability, and the λ_C follows the same rule.

Fig. 10 shows the control role simulation for the loading strategy group 1 measured by $RTCF_{global,l=n}$. The six simulation subfigures show $SUM^{Benchmark} > SUM^{LS\ 1\text{-}2} > SUM^{LS\ 1\text{-}1} > SUM^{LS\ 1\text{-}5} > SUM^{LS\ 1\text{-}4} > SUM^{LS\ 1\text{-}3}$ and $SUM_{\kappa}^{Benchmark} > SUM_{\kappa}^{LS\ 1\text{-}3} > SUM_{\kappa}^{LS\ 1\text{-}1} > SUM_{\kappa}^{LS\ 1\text{-}5} > SUM_{\kappa}^{LS\ 1\text{-}2} > SUM_{\kappa}^{LS\ 1\text{-}4}$, indicating that loading the SEC can effectively improve the cascading reliability of the MPTS, and the optimization design for loading strategies can further improve the control efficiency. In addition, there are some differences among the evolutions of SUM, SUM_{κ}, and RCF: (i) in terms of SUM_{κ}, the LS 1-4 has the best control capability of the interdependent cascading failures, which is in line with the results of RCF; (ii) in terms of SUM, the LS 1-3 has the best control capability of the interdependent cascading failures. The reason is that there is $\lambda_c^{LS\ 1\text{-}4} > \lambda_c^{LS\ 1\text{-}3}$, i.e., the LS 1-3 can quickly achieve a significant increase in cascading reliability, making the evolution of SUM under the two loading strategies significantly different in the simulation interval $\lambda \in [\lambda_c^{LS\ 1\text{-}3}, \lambda_c^{LS\ 1\text{-}4}]$ to eventually cause $SUM^{LS\ 1\text{-}4} > SUM^{LS\ 1\text{-}3}$. However, the SUM of LS 1-4 is much smaller than that of LS 1-3 outside the simulation interval $\lambda \in [\lambda_c^{LS\ 1\text{-}3}, \lambda_c^{LS\ 1\text{-}4}]$, which can be found together with Fig. 9. Therefore, in summary, LS 1-4 has the best control capability of the interdependent cascading failures in most simulation intervals.

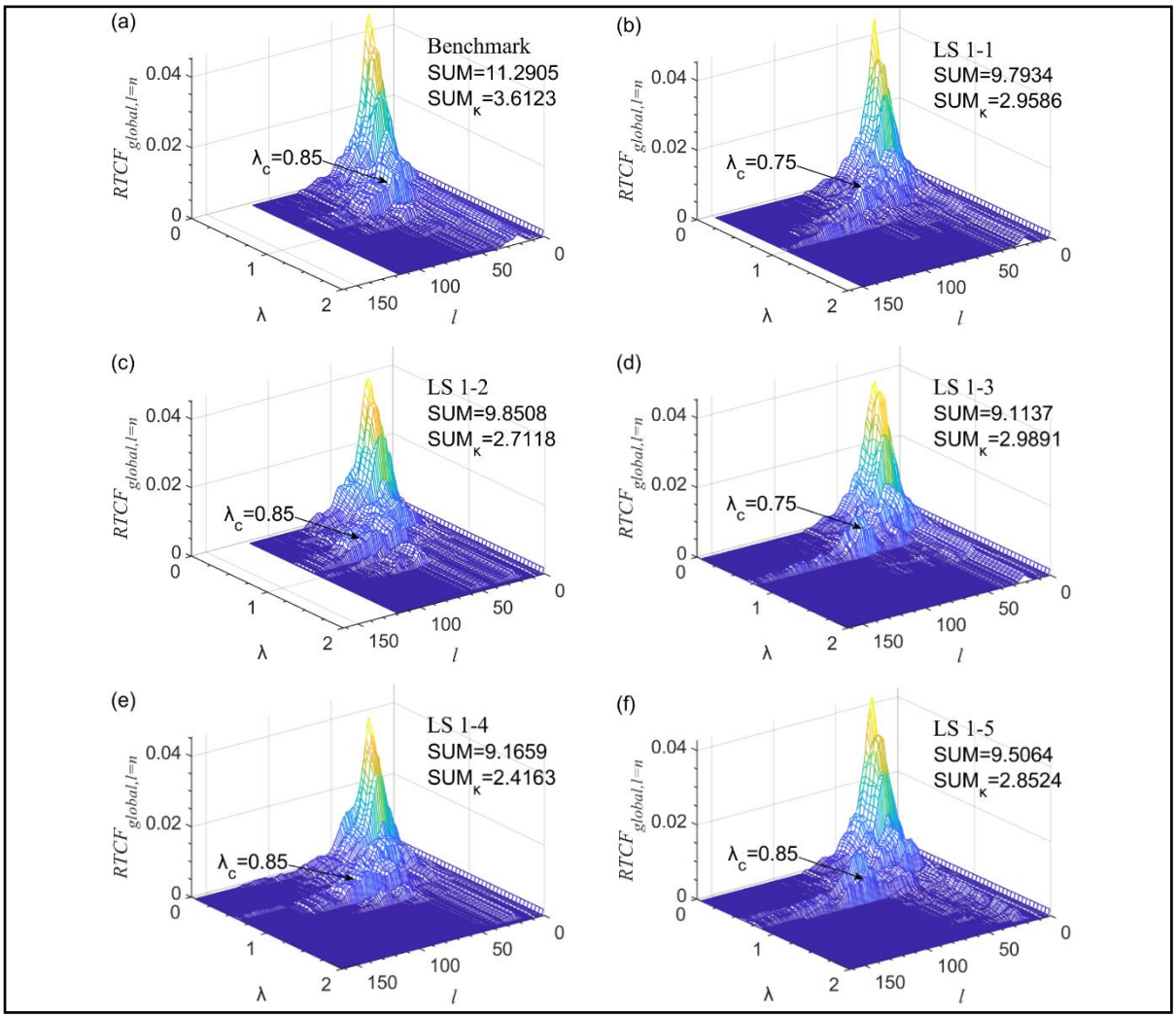

Fig. 10. Simulation results of the loading strategy group 1 measured by $RTCF_{global,l=n}$.

Simulation results measured by $RTCF_{local,l=n}$

$RTCF_{local,l=n}$ is the ratio between the number of failure stations and the number of stations that can be affected by cascading failures in the time-step $l=n$. The smaller the $RTCF_{local,l=n}$ of a point, the greater the local cascading reliability, and the λ_C follows the same rule.

Fig. 11 shows the control role simulation for the loading strategy group 1 measured by $RTCF_{local,l=n}$. The six simulation subfigures show that $SUM^{Benchmark} > SUM^{LS\ 1\text{-}2} > SUM^{LS\ 1\text{-}1} > SUM^{LS\ 1\text{-}5} > SUM^{LS\ 1\text{-}4} > SUM^{LS\ 1\text{-}3}$, which is in line with the results of SUM in Fig. 10. This observation indicates that loading the SEC can effectively improve the local cascading reliability of the MPTS and the optimization design for loading strategies works well. However, similar to the insights obtained from Fig. 10, the LS 1-3 instead of the LS 1-4 shows the best performance on SUM. This may be attributed to the differential evolution of the black dashed area in Fig. 11(e), which also covers the special simulation interval $\lambda \in [\lambda_c^{LS\ 1\text{-}3}, \lambda_c^{LS\ 1\text{-}4}]$ and

further illustrates the importance of identifying the optimally applicable simulation interval for different loading strategies.

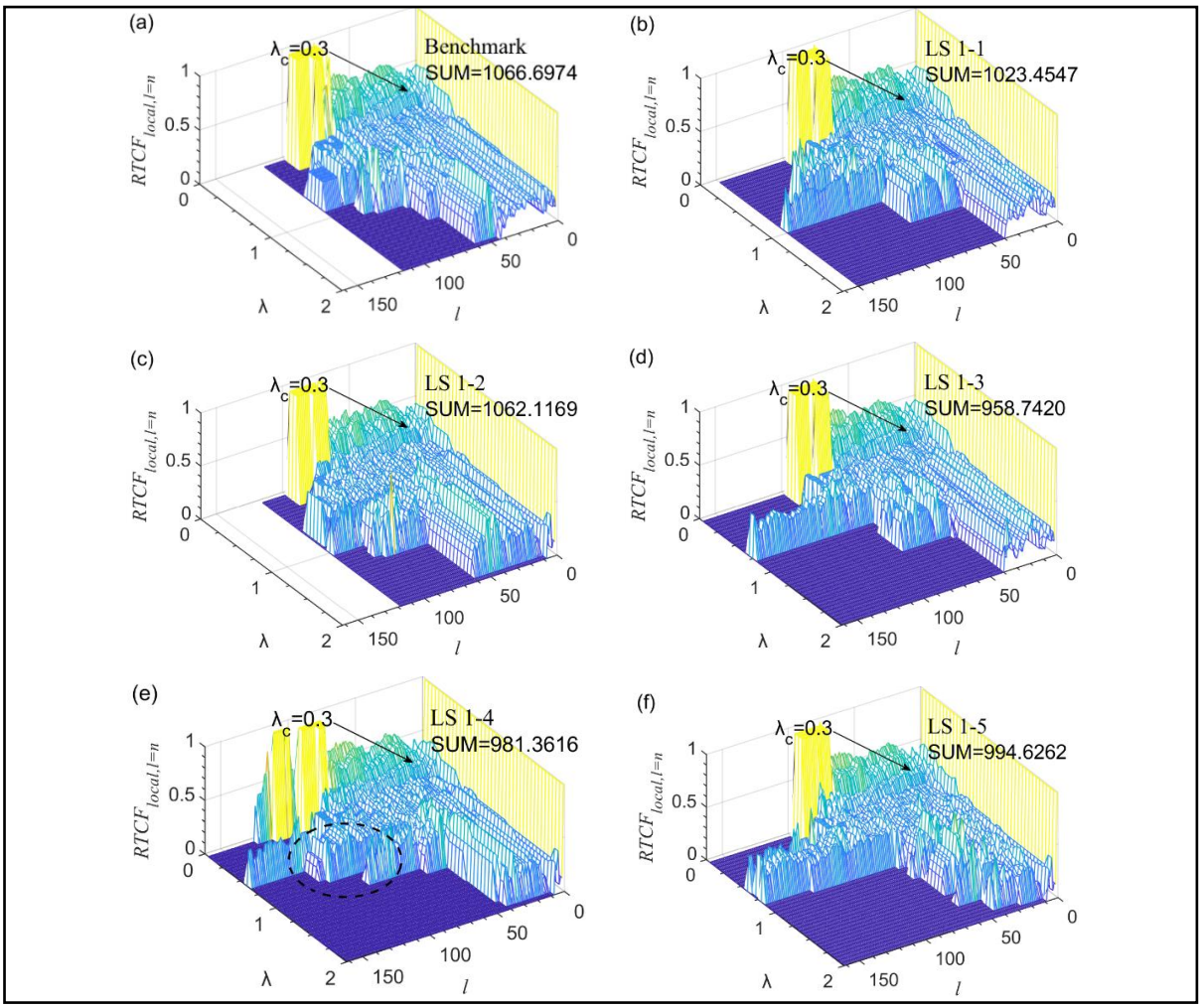

Fig. 11. Simulation results of the loading strategy group 1 measured by $RTCF_{local,l=n}$.

Simulation results measured by $LTCF_{l=n}$

$LTCF_{l=n}$ is the arithmetic mean of the load loss ratios of three layers in the time-step $l=n$. This type of load contains the paralyzed load (redistributed failure load) with no adjacent stations to redistribute and the failure load that exceeds the limit value for the redistributable failure load of failure stations in a single time-step. The smaller the $LTCF_{l=n}$ of a point, the greater the evacuation pressure from accumulated failure loads. In particular, as we tested in the previous work [31], $LTCF_{l=n}$ is an unstable evaluation indicator for measuring cascading reliability. Thus, $LTCF_{l=n}$ will only serve as a supporting indicator for the other three indicators, which also align with the primary purpose of this study, i.e., blocking the dynamic unfolding of the interdependent cascading failures as soon as possible.

Fig. 12 shows the control role simulation for the loading strategy group 1 measured by $LTCF_{l=n}$. The six simulation subfigures show that $SUM^{Benchmark} > SUM^{LS\ 1\text{-}2} > SUM^{LS\ 1\text{-}4} > SUM^{LS\ 1\text{-}5} > SUM^{LS\ 1\text{-}1} > SUM^{LS\ 1\text{-}3}$, which indicates that loading the SEC can effectively reduce the number of paralyzed loads and the evacuation pressure from accumulated failure loads. The paralyzed loads under the LS 1-2 and LS 1-4 are much larger, implying that the loading strategies designed based on the stations with smaller capacity sacrifice the transportability of part of the loads. While the LS-1-4 performs well in the three aspects above, the transportability of the load should be balanced against these aspects. Accordingly, this finding further suggests that the control efficiency of different loading strategies should be comprehensively evaluated from multiple perspectives.

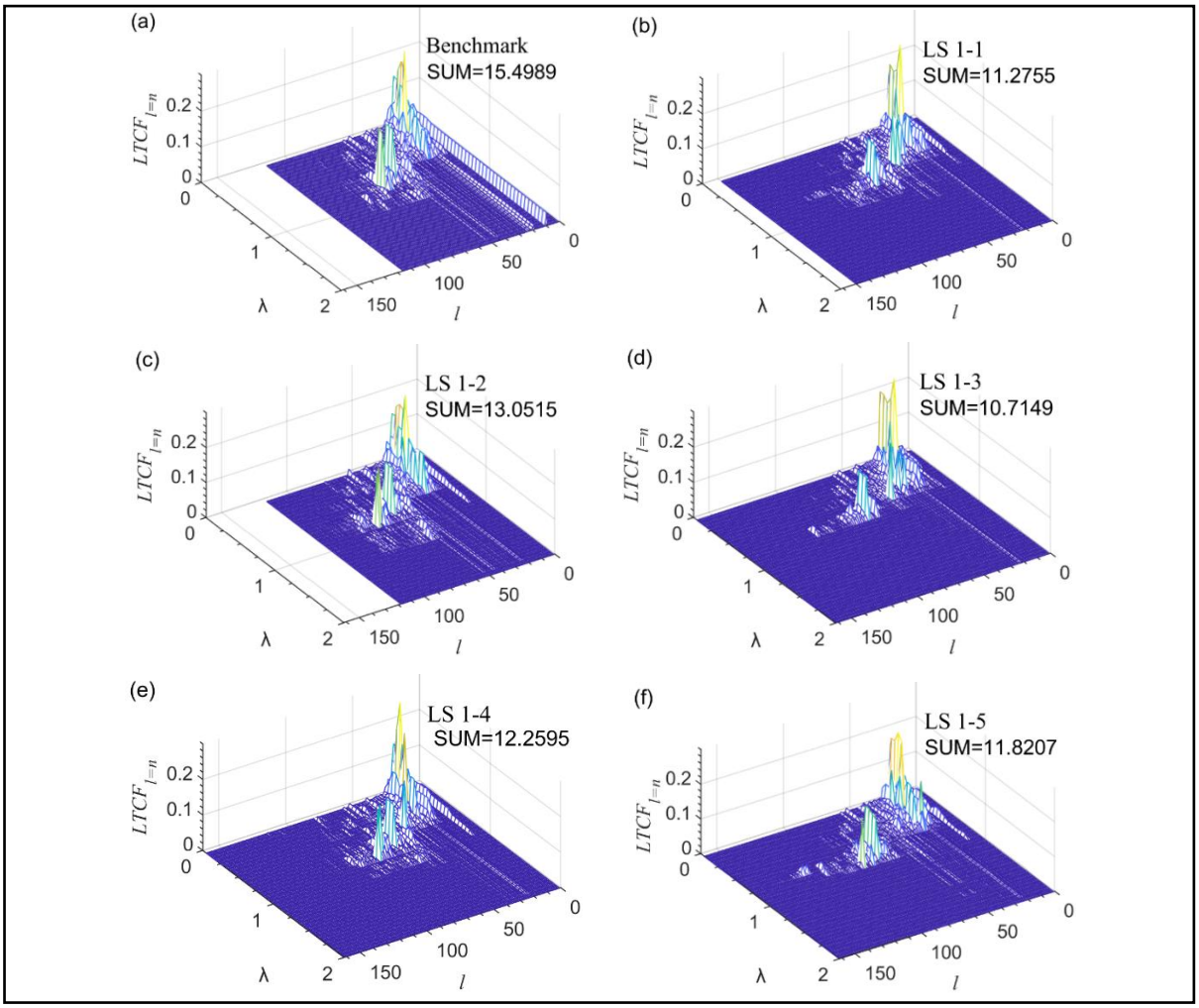

Fig. 12. Simulation results of the loading strategy group 1 measured by $LTCF_{l=n}$.

Critical insights from simulations of the loading strategy group 1

The LS 1-4, i.e., the loading strategy designed based on the stations with smaller capacity, has the optimal control capability of the interdependent cascading failures in most simulation intervals. However, it sacrifices the transportability of some loads compared to other loading

strategies. The LS 1-3, i.e., the loading strategy designed based on the stations with larger capacity, only has the optimal control capability of the interdependent cascading failures in a small simulation interval. However, it has a smaller (better) λ_c to control the spread of cascading failures rapidly. Therefore, in real-world operations, public transit managers should allocate emergency resources to the stations with smaller capacity in dynamic unfolding paths; and only in a few specific cases with the parameter λ falling in $[\lambda_c^{LS\ 1\text{-}3}, \lambda_c^{LS\ 1\text{-}4}]$, the allocation targets should be the stations with larger capacity. In addition, the above results also shed light on the future real-time control optimization for cascading failures with advanced intelligent algorithms. The simulations of Group 1 are induced by a sudden large passenger flow from the Nanjing Station, i.e., the unfolding of cascading failures is triggered by the failure of a large hub station. However, the unexpected failures of non-hub stations are more common in real-world operations, and their unpredictability will significantly increase the difficulty of controlling cascading failures. Therefore, combined with the swarm intelligence algorithm, the simulations of Group 1 help develop advanced intelligent algorithms to identify the optimal SEC loading way in the single time-step scale under unexpected failures.

5.2. The control role simulation for the loading strategy group 2

In this subsection, the loading time-step intervals of the LS 2-1, LS 2-2, and LS 2-3 are specified as $l \in [2,9]$, $l \in [10,17]$, and $l \in [18,25]$, respectively. The loading way in a single time-step is specifically as the LS 1-4. In each time-step of the specified intervals, one station of the lower layer, two stations of the middle layer, and one station of the upper layer are loaded with the SEC equal to the $SEC_{baseline}^{lower}$, $SEC_{baseline}^{middle}$, and $SEC_{baseline}^{upper}$, respectively.

Simulation results measured by RCF

Fig. 13 shows the control role simulation for the loading strategy group 2 measured by RCF. The four evolution curves have the same λ_C, indicating that changing the loading time-step intervals to load the SEC cannot effectively optimize the λ_C. In addition, the LS 2-2 has the optimal control capability of the interdependent cascading failures in the simulation interval $\lambda \in [0.35, 0.8]$, and the LS 2-3 has the optimal control capability in most of the rest of the simulation intervals, which suggests that loading the SEC in the initial time-steps of cascading failures has a lower control efficiency. The reason is that the unfolding of failure loads is gathered in a limited scope in the initial time-steps of cascading failures, and the excessively gathered failure loads reduce the adjusting capability provided by the SEC on the station state and cascading failure scale.

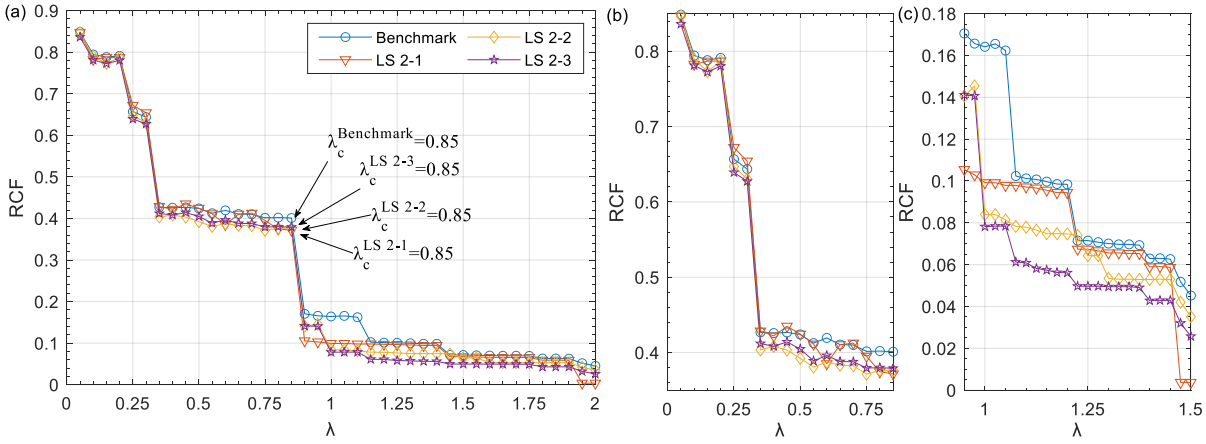

Fig. 13. Simulation results of the loading strategy group 2 measured by RCF.

Simulation results measured by $RTCF_{global,l=n}$

Fig. 14 shows the control role simulation for the loading strategy group 2 measured by $RTCF_{global,l=n}$. The four simulation subfigures show that $SUM^{Benchmark} > SUM^{LS\ 2\text{-}1} > SUM^{LS\ 2\text{-}2} > SUM^{LS\ 2\text{-}3}$ and $SUM_{\kappa}^{Benchmark} > SUM_{\kappa}^{LS\ 2\text{-}1} > SUM_{\kappa}^{LS\ 2\text{-}2} > SUM_{\kappa}^{LS\ 2\text{-}3}$, indicating that in terms of overall evolution, the LS 2-3 has the optimal control capability of the interdependent cascading failures. In particular, the loading time-step interval of the LS 2-3 is $l \in [18, 25]$, which has a large overlap with the time-step interval of the area κ, in which the MPTS has the largest failure strength under the natural unfolding of cascading failures. Accordingly, we can conclude that the SEC should be loaded in the time-steps where the MPTS has the largest failure strength.

Simulation results measured by $RTCF_{local,l=n}$

Fig. 15 presents the simulation results of the loading strategy group 2 measured by $RTCF_{local,l=n}$. The four simulation subfigures show $SUM^{Benchmark} > SUM^{LS\ 2\text{-}1} > SUM^{LS\ 2\text{-}3} > SUM^{LS\ 2\text{-}2}$, indicating that in terms of overall evolution, the LS 2-2 has the optimal control capability of the local cascading failures. It should be emphasized that different from the optimal capability of the LS 2-3 regarding $RTCF_{global,l=n}$, the LS 2-2 has the optimal capability regarding $RTCF_{local,l=n}$. The reason is that as the cascading failures continue to unfold, the number of failure stations in each time-step becomes larger than the fixed number of the loadable SEC. Therefore, the loading strategies should be comprehensively evaluated from multiple perspectives as much as possible so as to adapt to different needs and concerns in varying real-time cases.

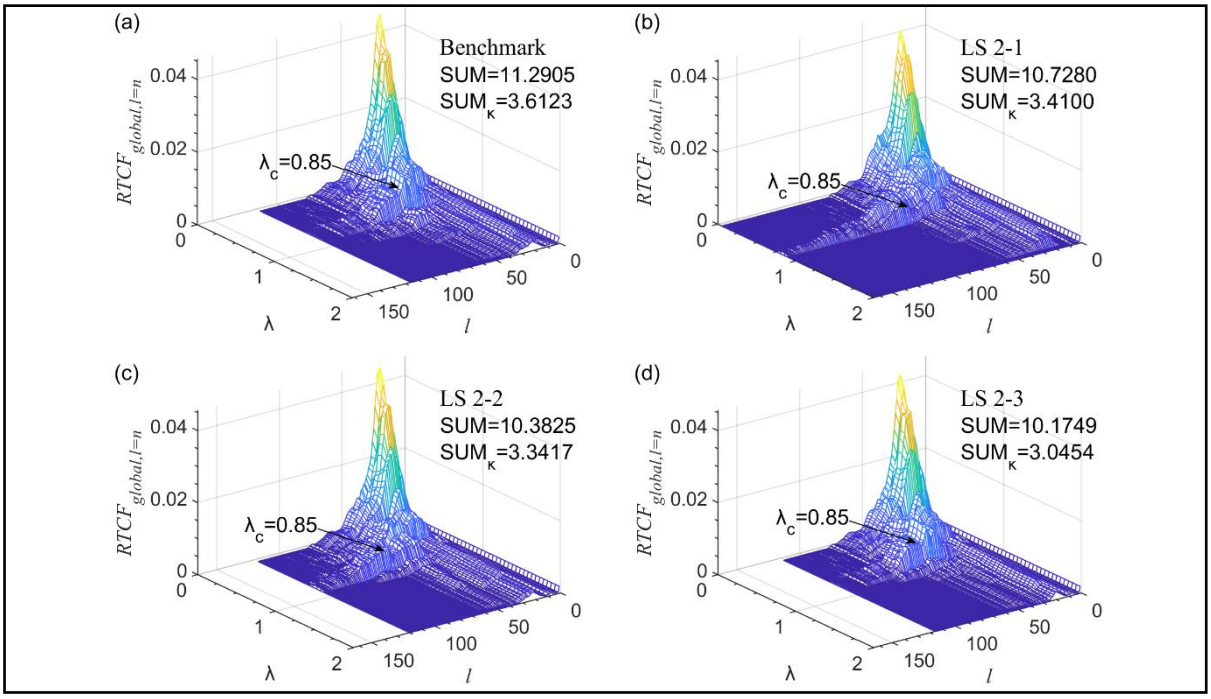

Fig. 14. Simulation results of the loading strategy group 2 measured by $RTCF_{global,l=n}$.

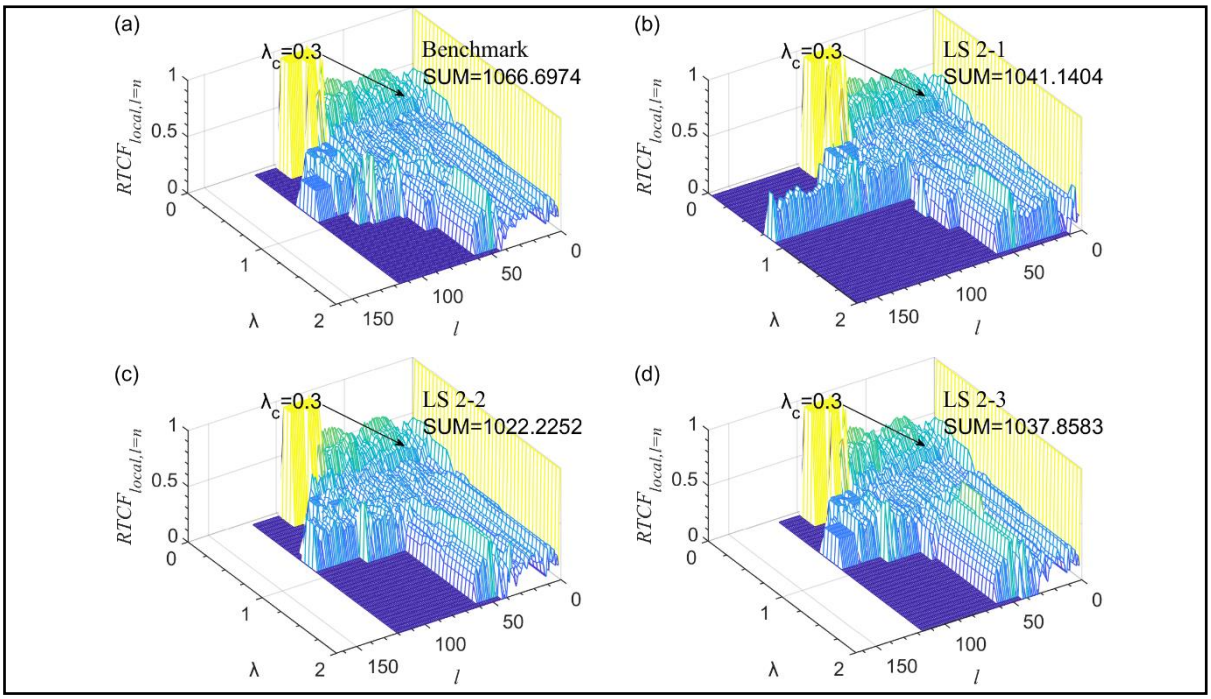

Fig. 15. Simulation results of the loading strategy group 2 measured by $RTCF_{local,l=n}$.

Simulation results measured by $LTCF_{l=n}$

Fig. 16 presents the control role simulation for the loading strategy group 2 measured by $LTCF_{l=n}$. The four simulation subfigures show $SUM^{Benchmark} > SUM^{LS\ 2\text{-}3} > SUM^{LS\ 2\text{-}2} > SUM^{LS\ 2\text{-}1}$, indicating that the loading strategy group 2 can effectively reduce the number of paralyzed loads and the evacuation pressure from accumulated failure loads. In particular, the

LS 2-1 performs best in reducing the number of paralyzed loads. Combining the conclusions obtained in Figs. 13-15 and the fact that the loading time-step intervals of the LS 2-2 and LS 2-3 are both non-initial time-steps, it can be concluded that the control capability of the interdependent cascading failures can be improved by conducting the delayed responses at the sacrifice of the transportability of some loads.

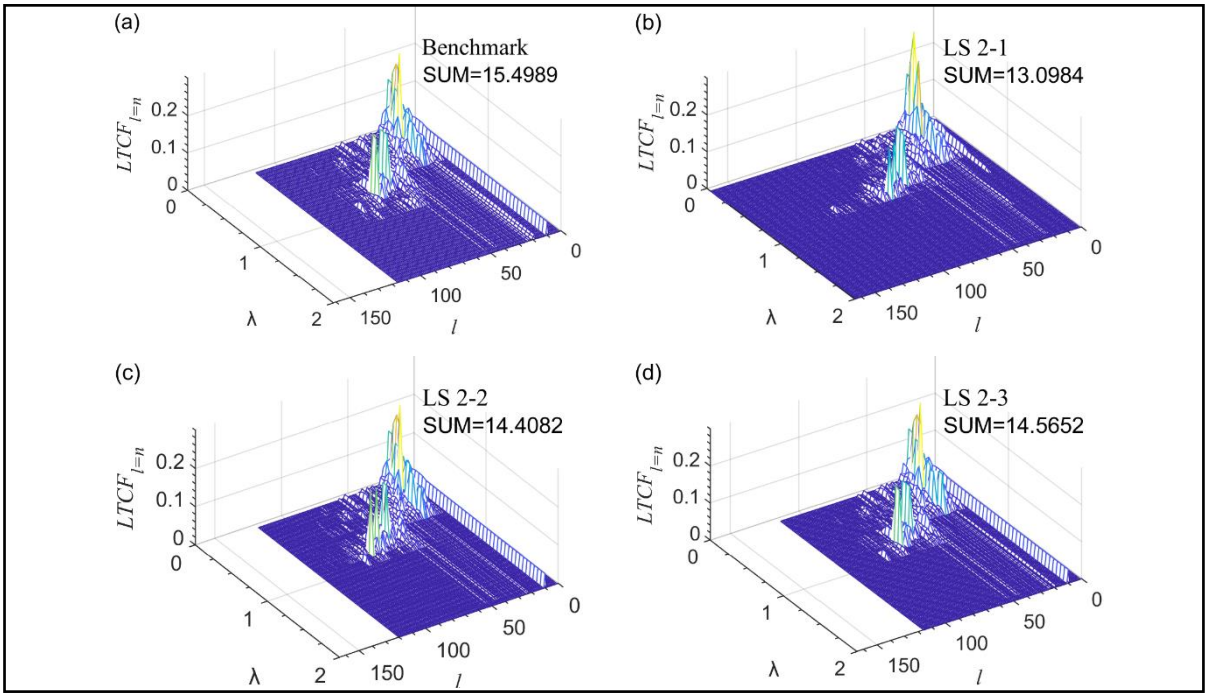

Fig. 16. Simulation results of the loading strategy group 2 measured by $LTCF_{l=n}$.

Critical insights from simulations of the loading strategy group 2

Loading the SEC by avoiding the initial time-steps can further improve the control efficiency of the local and global cascading failures. When the delayed responses are conducted in the time-steps in which the MPTS has the largest failure strength, i.e., the LS 2-3, the dynamic unfolding of cascading failures can be best blocked at the sacrifice of the transportability of some loads. Therefore, in real-world operations, public transit managers should allocate emergency resources in the time-steps that intersect as much as possible with the time-steps in which the MPTS has the largest failure strength, rather than the initial time-steps. In addition, the simulations of Group 2 also show that the delayed responses should have a boundary because the cascading failure scale of stations and the sacrificing transportability of loads will be accelerated in the later time-steps. Particularly, the sacrificing transportability of loads should be treated as a more critical optimization metric than that for blocking the dynamic unfolding of cascading failures. Therefore, multi-objective optimization solutions for an accurate boundary of delayed responses should be developed by resorting to intelligent optimization algorithms in the future.

5.3. The control role simulation for the loading strategy group 3

In this subsection, the LS 3-1 and LS 3-2 are both developed from the LS 2-2, i.e., the loading time-step interval is $l \in [10,13]$, and the SEC that originally belongs to the time-step interval $l \in [14,17]$ is loaded to the 'unplanned stations' or 'planned stations' in the time-step interval $l \in [10,13]$. Besides, the loading way in a single time-step is also the LS 1-4. Therefore, regarding the LS 3-1, two stations of the lower layer, four stations of the middle layer, and two stations of the upper layer are loaded with the SEC equal to the $SEC_{baseline}^{lower}$, $SEC_{baseline}^{middle}$, and $SEC_{baseline}^{upper}$ in each time-step of the specified interval, respectively. As for the LS 3-2, one station of lower layer, two stations of the middle layer, and one station of the upper layer are loaded with the SEC equal to the $2 \cdot SEC_{baseline}^{lower}$, $2 \cdot SEC_{baseline}^{middle}$, and $2 \cdot SEC_{baseline}^{upper}$ in each time-step of the specified interval, respectively.

Simulation results measured by RCF

Fig. 17 shows the control role simulation for the loading strategy group 3 measured by *RCF*. The four evolution curves have the same λ_C, indicating that shortening the loading interval length and increasing the loading strength cannot effectively optimize the λ_C. In addition, the LS 2-2 has the optimal control capability of the interdependent cascading failures in most simulation intervals, implying that shortening the loading interval length and increasing the loading strength will reduce the SEC control efficiency when the total SEC is fixed. The reason is that the centralized SEC loading within a short time-step interval may prevent part of the SEC from participating in reducing the evacuation pressure of failure loads.

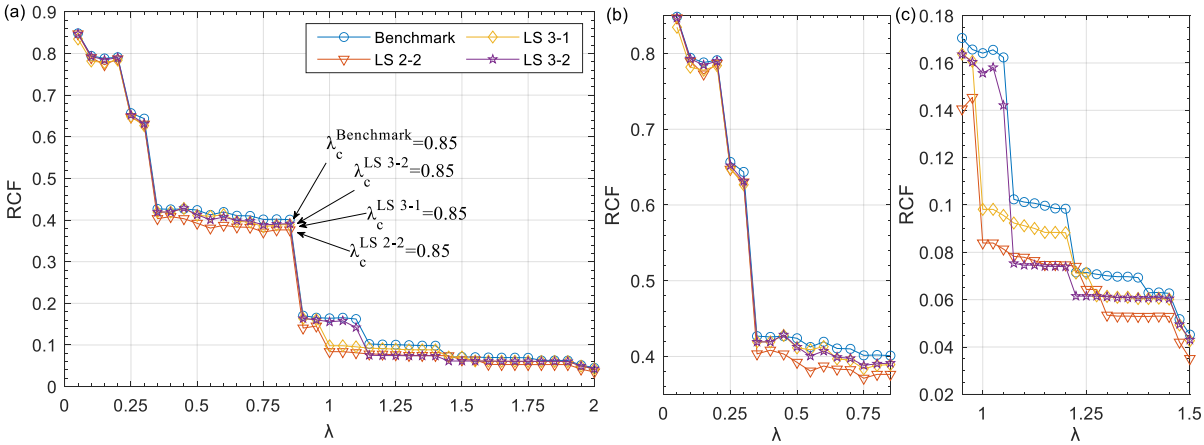

Fig. 17. Simulation result of the loading strategy group 3 measured by *RCF*.

Simulation results measured by $RTCF_{global,l=n}$

Fig. 18 presents the control role simulation for the loading strategy group 3 measured by $RTCF_{global,l=n}$. The four simulation subfigures show that $SUM^{Benchmark} > SUM^{LS\ 3\text{-}2} > SUM^{LS\ 3\text{-}1} > SUM^{LS\ 2\text{-}2}$ and $SUM_{\kappa}^{Benchmark} > SUM_{\kappa}^{LS\ 3\text{-}1} > SUM_{\kappa}^{LS\ 3\text{-}2} > SUM_{\kappa}^{LS\ 2\text{-}2}$, indicating that in terms of overall evolution, the LS 2-2 has the optimal control capability of the interdependent cascading failures, which is in line with the results of RCF. In other words, shortening the loading interval length and increasing the loading strength cannot improve the cascading reliability when the total SEC is fixed.

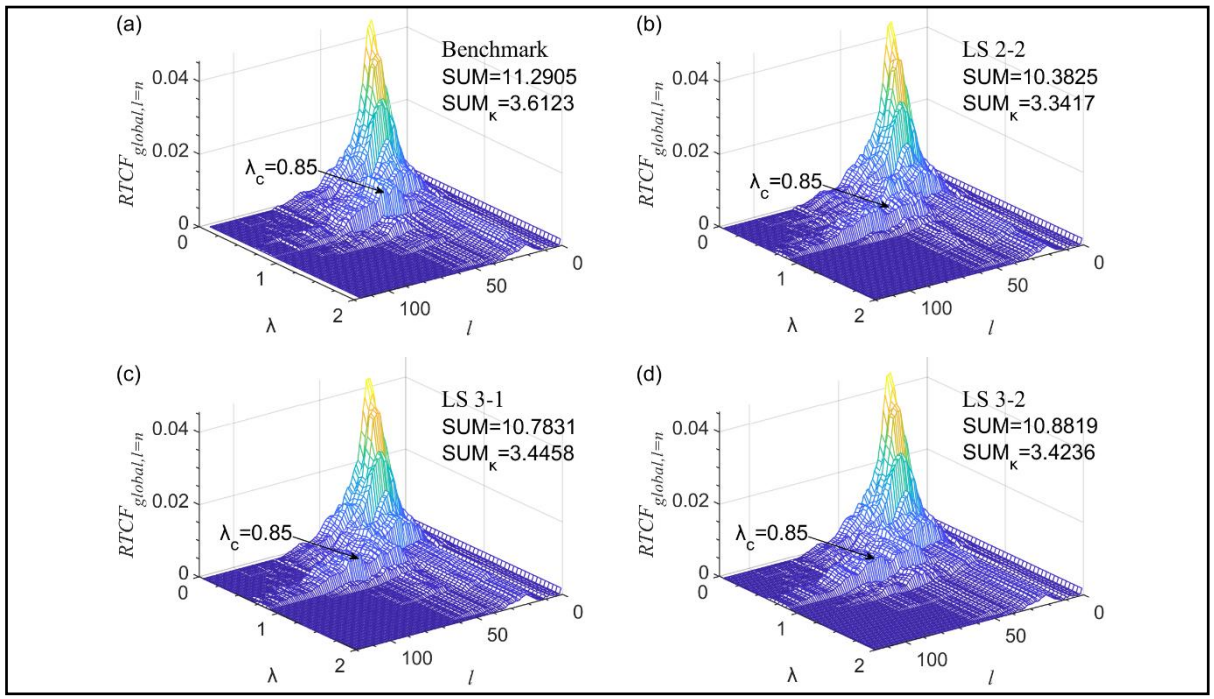

Fig.18. Simulation results of the loading strategy group 3 measured by $RTCF_{global,l=n}$.

Simulation results measured by $RTCF_{local,l=n}$

Fig. 19 presents the control role simulation for the loading strategy group 3 measured by $RTCF_{local,l=n}$. The four simulation subfigures show that $SUM^{Benchmark} > SUM^{LS\ 3\text{-}2} > SUM^{LS\ 3\text{-}1} > SUM^{LS\ 2\text{-}2}$, indicating that in terms of overall evolution, the LS 2-2 has the optimal control capability of local cascading failures. In other words, shortening the loading interval length and increasing the loading strength will reduce the SEC control efficiency when the total SEC is fixed.

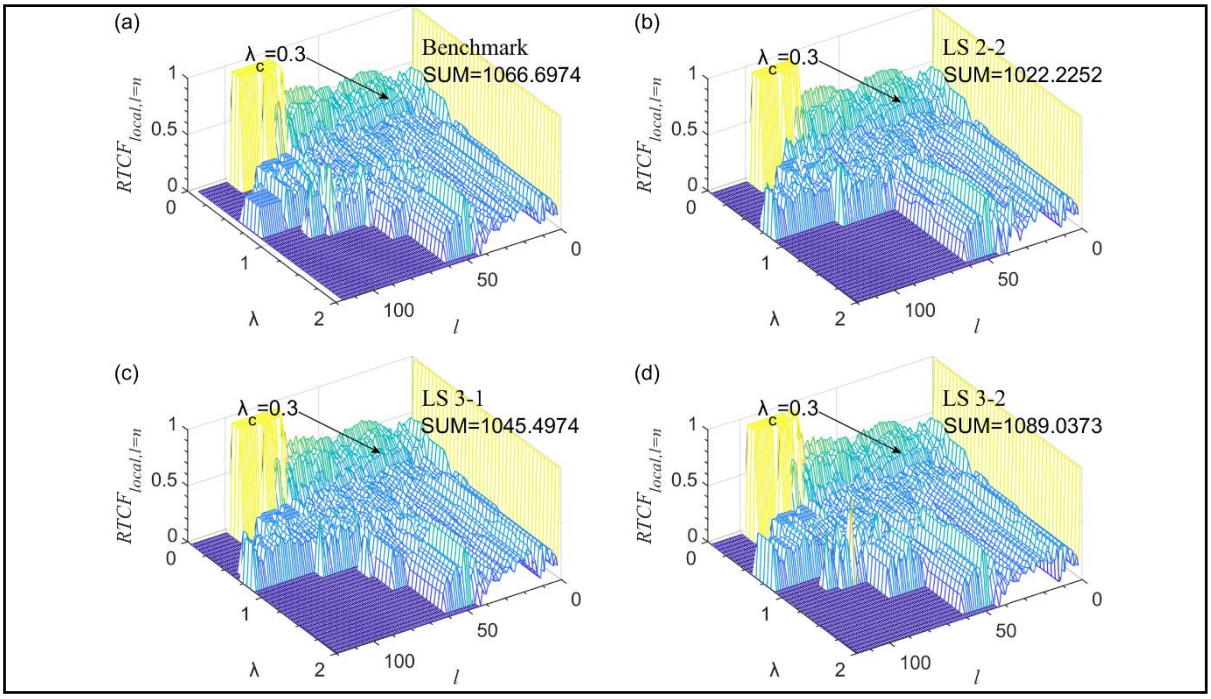

Fig. 19. Simulation results of the loading strategy group 3 measured by $RTCF_{local,l=n}$.

Simulation results measured by $LTCF_{l=n}$

Fig. 20 presents the control role simulation results for the loading strategy group 3 measured by $LTCF_{l=n}$. The four simulation subfigures show $SUM^{Benchmark} > SUM^{LS\ 3\text{-}2} > SUM^{LS\ 3\text{-}1} > SUM^{LS\ 2\text{-}2}$, indicating that the LS 2-2 has the best performance in reducing the number of paralyzed loads and the evacuation pressure from accumulated failure loads. The finding is consistent with the conclusions obtained in Figs. 17-19. Therefore, the SEC control efficiency can be improved by continuously loading the SEC in a longer time-step interval rather than centrally loading the SEC in a shorter time-step interval.

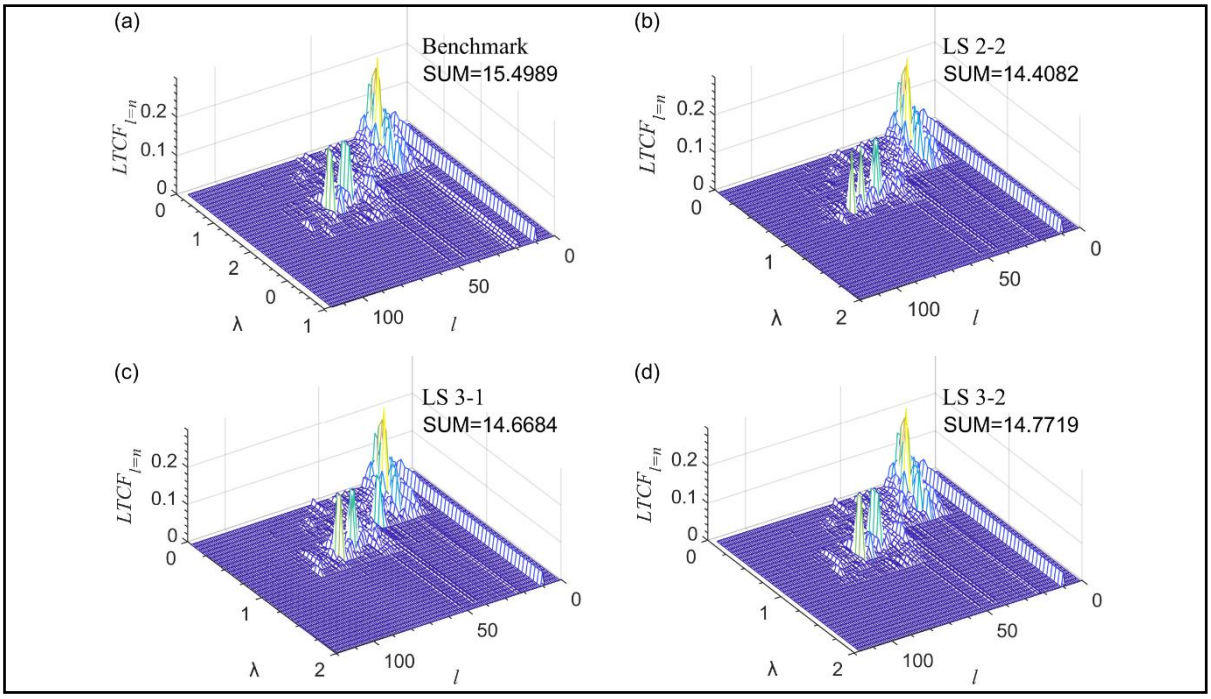

Fig. 20. Simulation results of the loading strategy group 3 measured by $LTCF_{l=n}$.

Critical insights from simulations of the loading strategy group 3

When the total SEC is fixed, shortening the loading interval length and increasing the loading strength cannot effectively control the local and global cascading failures and reduce the number of paralyzed loads and the evacuation pressure from accumulated failure loads. In a nutshell, this operation will reduce the SEC control efficiency. Therefore, in real-world operations, public transit managers should allocate emergency resources in a longer time-step interval rather than concentrate emergency resources in a shorter time-step interval. In addition, the efficiency of Group 3 may significantly change if the scale of failure loads in each unfolding path becomes large enough. Note that the failure scale depends on the limit value of the redistributable failure load originating from a failure station [31]. Therefore, regarding the insights for algorithm-based optimal control, the simulations of Group 3 can guide the determination of the optimal numerical simulation combination of the SEC baseline value, the loading interval length and loading strength, and the limit value of the redistributable failure load originating from a failure station.

6. Conclusion and future work

The interdependent cascading failures caused by a sudden large passenger flow will largely affect the operating efficiency and resilience of sustainable public transit and road infrastructure. The vulnerability of an MPTS against this severe failure, associated with extreme performances, limits the building of future resilient megacities. Most existing studies

on cascading failure controls focused on qualitative optimization strategies for long-term network designs at a strategic level rather than conducting real-time operational controls to mitigate negative impacts. This paper proposes a real-time operational control method based on the SEC to quickly block the dynamic unfolding paths of this severe failure considering network topology characteristics and dynamic evolution characteristics. To explore the most efficient SEC loading strategy, a three-stage association design process involves multiple intertwined influential factors, including the target loading stations, loading time-step intervals, and loading interval length and loading strength. Finally, a case simulation is conducted to verify the adaptability of the proposed method, which provides critical insights into real-world emergency resource allocation and an underlying simulator with search direction knowledge for future intelligent algorithm-based optimal control.

The simulation results indicate that (i) the SEC should be allocated to the stations with smaller capacity in dynamic unfolding paths; (ii) the SEC should be allocated in the time-steps that intersect as much as possible with the time-steps in which MPTS has the largest failure strength, rather than the initial time-steps; (iii) the SEC should be continuously allocated in a long time-step interval rather than centrally allocated in a short time-step interval. These results serve as a crucial foundation for public transit managers in formulating efficient SEC loading strategies against interdependent cascading failures induced by a sudden large passenger. This aspect holds significant importance for the development of future cities, as it necessitates thoughtful contemplation of extreme performance scenarios when constructing resilient urban lifeline infrastructure within megacities, which encounter complex challenges in managing mixed environments with large populations and interdependent cascading failures.

Although considering the intertwined factors for designing the SEC loading strategies has contributed to exploring the most efficient SEC loading mechanism, they may not cover all real-time cases in real-world engineering. In the future, guided by the obtained search direction knowledge and the underlying simulator, an intelligent algorithm-based optimal control method can be developed to significantly improve computational efficiency and intelligence of various large-scale and complex problems under unexpected failures.

Conflicts of interest

The authors declare that they have no conflicts of interest.

Acknowledgements

This work was supported by the National Natural Science Foundation of China [Grant Nos. 72071173, 72371221, 72361137006], and the Research Grants Council of the Hong Kong Special Administrative Region, China [Project number HKSAR RGC TRS T32-707/22-N].

Appendix

A.1. Acronyms

FLDR	failure load dynamic redistribution
LS 1-1	Loading Strategy 1-1
MPTS	multimodal public transit system
SEC	system emergency capability

A.2. Notations

$C_{v_i}^{lower}$	the capacity of station v_i in the lower layer
$C_{v_i'}^{middle}$	the capacity of station v_i' in the middle layer
$C_{v_i''}^{upper}$	the capacity of station v_i'' in the upper layer
$L_{v_{j3},l=n+1}$	the carrying load of station v_{j3} at the beginning point of time-step $l=n+1$
$LTCF_{l=n}$	the arithmetic mean of the load loss ratios of three layers in the time-step $l=n$
N^{lower}	the number of stations in the lower layer
N^{middle}	the number of stations in the middle layer
N^{upper}	the number of stations in the upper layer
RCF	the ratio between the number of failure stations and the number of stations in the MPTS
$RTCF_{global,l=n}$	the ratio between the number of failure stations in the time-step $l=n$ and the number of stations in the MPTS
$RTCF_{local,l=n}$	the ratio between the number of failure stations and the number of stations that can be affected by cascading failures in the time-step $l=n$

$SEC_{baseline}^{lower}$	the SEC baseline value of the lower layer
$SEC_{baseline}^{middle}$	the SEC baseline value of the middle layer
$SEC_{baseline}^{upper}$	the SEC baseline value of the upper layer
SEC_{total}^{lower}	the total SEC of the lower layer
SEC_{total}^{middle}	the total SEC of the middle layer
SEC_{total}^{upper}	the total SEC of the upper layer
SUM	the sum of the z-axis values of a figure
SUM_{κ}	the sum of the z-axis values of the area κ of a figure (area κ follows $\lambda \in [0,2] \wedge l \in [20,30]$)
λ	the load tolerance parameter
λ_C	the threshold of the parameter λ
$\Delta L_{v_i \to v_{j3}, l=n}$	the failure load redistributed from the failure station v_i to the adjacent station v_{j3} in the time-step $l = n$

References

[1]. Yun, Z., et al., Paths and strategies for a resilient megacity based on the water-energy-food nexus. Sustainable Cities and Society, 2022. 82: p. 103892.

[2]. Lara, D.V.R., P. Pfaffenbichler and A.N. Rodrigues Da Silva, Modeling the resilience of urban mobility when exposed to the COVID-19 pandemic: A qualitative system dynamics approach. Sustainable Cities and Society, 2023. 91: p. 104411.

[3]. Chu, Z., M. Cheng and M. Song, What determines urban resilience against COVID-19: City size or governance capacity? Sustainable Cities and Society, 2021. 75: p. 103304.

[4]. Dong, S., et al., Probabilistic modeling of cascading failure risk in interdependent channel and road networks in urban flooding. Sustainable Cities and Society, 2020. 62: p. 102398.

[5]. Moazeni, F. and J. Khazaei, Formulating false data injection cyberattacks on pumps' flow rate resulting in cascading failures in smart water systems. Sustainable Cities and Society, 2021. 75: p. 103370.

[6]. Duan, J., D. Li and H. Huang, Reliability of the traffic network against cascading failures with individuals acting independently or collectively. Transportation Research Part C:

Emerging Technologies, 2023. 147: p. 104017.
[7]. Guo, X., et al., Cascading failure and recovery of metro–bus double-layer network considering recovery propagation. Transportation Research Part D: Transport and Environment, 2023. 122: p. 103861.
[8]. Zhang, L., M. Xu and S. Wang, Quantifying bus route service disruptions under interdependent cascading failures of a multimodal public transit system based on an improved coupled map lattice model. Reliability Engineering & System Safety, 2023. 235: p. 109250.
[9]. Dong, Z., et al., Mitigating cascading failures of spatially embedded cyber–physical power systems by adding additional information links. Reliability Engineering & System Safety, 2022. 225: p. 108559.
[10]. Wang, Z., et al., Cascading risk assessment in power-communication interdependent networks. Physica A: Statistical Mechanics and its Applications, 2020. 540: p. 120496.
[11]. Ma, F., et al., Exploring the robustness of public transportation for sustainable cities: a double-layered network perspective. Journal of Cleaner Production, 2020. 265: p. 121747.
[12]. Chen, H., et al., Simulation-based vulnerability assessment in transit systems with cascade failures. Journal of Cleaner Production, 2021. 295: p. 126441.
[13]. Liu, Z., et al., Evaluating the dynamic resilience of the multi-mode public transit network for sustainable transport. Journal of Cleaner Production, 2022. 348: p. 131350.
[14]. Huang, Z. and B.P.Y. Loo, Vulnerability assessment of urban rail transit in face of disruptions: A framework and some lessons from Hong Kong. Sustainable Cities and Society, 2023. 98: p. 104858.
[15]. Tan, Z., et al., Evacuating metro passengers via the urban bus system under uncertain disruption recovery time and heterogeneous risk-taking behaviour. Transportation Research Part C: Emerging Technologies, 2020. 119: p. 102761.
[16]. Estrada, M., et al., Bus control strategies in corridors with signalized intersections. Transportation Research Part C: Emerging Technologies, 2016. 71: p. 500-520.
[17]. Barabási, A., Network Science. 2016: Cambridge University Press.
[18]. Sun, D. and S. Guan, Measuring vulnerability of urban metro network from line operation perspective. Transportation Research Part A: Policy and Practice, 2016. 94: p. 348-359.
[19]. Ma, F., et al., Assessing the vulnerability of urban rail transit network under heavy air pollution: a dynamic vehicle restriction perspective. Sustainable Cities and Society, 2020. 52: p. 101851.
[20]. Huang, W., et al., Using the disaster spreading theory to analyze the cascading failure of

urban rail transit network. Reliability Engineering & System Safety, 2021. 215: p. 107825.
[21].Lu, Q., et al., Modeling network vulnerability of urban rail transit under cascading failures: a coupled map lattices approach. Reliability Engineering & System Safety, 2022. 221: p. 108320.
[22].Shen, Y., G. Ren and B. Ran, Analysis of cascading failure induced by load fluctuation and robust station capacity assignment for metros. Transportmetrica A: Transport Science, 2022. 18(3): p. 1401-1419.
[23].Zhang, Y. and S.T. Ng, Robustness of urban railway networks against the cascading failures induced by the fluctuation of passenger flow. Reliability Engineering & System Safety, 2022. 219: p. 108227.
[24].Zhang, L., et al., A cascading failures model of weighted bus transit route network under route failure perspective considering link prediction effect. Physica A: Statistical Mechanics and its Applications, 2019. 523: p. 1315-1330.
[25].Zou, Z., Y. Xiao and J. Gao, Robustness analysis of urban transit network based on complex networks theory. Kybernetes, 2013. 42(3): p. 383-399.
[26].Zhang, L., B.B. Fu and Y.X. Li, Cascading failure of urban weighted public transit network under single station happening emergency. Procedia Engineering, 2016. 137: p. 259-266.
[27].Su, Z., et al., Robustness of interrelated traffic networks to cascading failures. Scientific Reports, 2014. 4: p. 5413.
[28].Yang, Y., A. Huang and W. Guan, Statistic properties and cascading failures in a coupled transit network consisting of bus and subway systems. International Journal of Modern Physics B, 2014. 28(30): p. 1450212.
[29].Shen, L., et al., Simulation on Survivability and Cascading Failure Propagation of Urban Subway-Bus Compound Network. Journal of Southwest Jiaotong University, 2018. 53(1): p. 156-163.
[30].Jo, S., et al., Cascading failure with preferential redistribution on bus–subway coupled network. International Journal of Modern Physics C, 2021. 32(8): p. 2150103.
[31].Zhang, L., et al., Exploring cascading reliability of multi-modal public transit network based on complex networks. Reliability Engineering & System Safety, 2022. 221: p. 108367.
[32].Holmgren, A.J., Using graph models to analyze the vulnerability of electric power networks. Risk Analysis, 2006. 26(4): p. 955-969.
[33].Li, J., et al., Network resilience assessment and reinforcement strategy against cascading

failure. Chaos, Solitons & Fractals, 2022. 160: p. 112271.

[34]. Xie, J., et al., Eradicating abrupt collapse on single network with dependency groups. Chaos: An Interdisciplinary Journal of Nonlinear Science, 2019. 29(8): p. 083111.

[35]. Yuan, X., et al., Eradicating catastrophic collapse in interdependent networks via reinforced nodes. Proceedings of the National Academy of Sciences, 2017. 114(13): p. 3311-3315.

[36]. Zhang, L., et al., A quantitatively controllable mesoscopic reliability model of an interdependent public transit network considering congestion, time-delay interaction and self-organization effects. Nonlinear Dynamics, 2019. 96(2): p. 933-958.

[37]. Motter, A.E. and Y.C. Lai, Cascade-based attacks on complex networks. Physical Review E: Statistical Nonlinear & Soft Matter Physics, 2002. 66(2): p. 065102.

[38]. Mattsson, L. and E. Jenelius, Vulnerability and resilience of transport systems-A discussion of recent research. Transportation Research Part A: Policy & Practice, 2015. 81: p. 16-34.

[39]. Liu, J., et al., Robustness of complex networks with an improved breakdown probability against cascading failures. Physica A: Statistical Mechanics and its Applications, 2016. 456: p. 302-309.

[40]. Feng, S., Y. Chen and M. Xin, Coordination passenger flow control model for metro under sudden large passenger flow. Journal of Harbin Institute of Technology, 2019. 51(2): p. 179-185.

[41]. Zhang, L., et al., Comparing the time-varying topology-based dynamics between large-scale bus transit and urban rail transit networks from a mesoscopic perspective. Nonlinear Dynamics, 2021. 106(1): p. 657-680.